Damage assessment for the 2018 lower East Rift Zone lava flows of Kīlauea volcano, Hawaiʻi

Elinor S. Meredith[1,2] · Susanna F. Jenkins[1,2] · Josh L. Hayes[1,3] · Natalia Irma Deligne[3,4] · David Lallemant[1,2] ·
Matthew Patrick[4] · Christina Neal[4,5]

Abstract

Cataloguing damage and its correlation with hazard intensity is one of the key components needed to robustly assess future risk and plan for mitigation as it provides important empirical data. Damage assessments following volcanic eruptions have been conducted for buildings and other structures following hazards such as tephra fall, pyroclastic density currents, and lahars. However, there are relatively limited quantitative descriptions of the damage caused by lava flows, despite the number of communities that have been devastated by lava flows in recent decades (e.g., Cumbre Vieja, La Palma, 2021; Nyiragongo, Democratic Republic of Congo, 2002 and 2021; Fogo, Cape Verde, 2014–2015). The 2018 lower East Rift Zone (LERZ) lava flows of Kīlauea volcano, Hawaiʻi, inundated 32.4 km^2 of land in the Puna District, including residential properties, infrastructure, and farmland. During and after the eruption, US Geological Survey scientists and collaborators took over 8000 aerial and ground photographs and videos of the eruption processes, deposits, and impacts. This reconnaissance created one of the largest available impact datasets documenting an effusive eruption and provided a unique opportunity to conduct a comprehensive damage assessment. Drawing on this georeferenced dataset, satellite imagery, and 2019 ground-based damage surveys, we assessed the pre-event typology and post-event condition of structures within and adjacent to the area inundated by lava flows during the 2018 LERZ eruption. We created a database of damage: each structure was assigned a newly developed damage state and data quality category value. We assessed 3165 structures within the Puna District and classified 1839 structures (58%) as destroyed, 90 structures (3%) as damaged, and 1236 (39%) as unaffected. We observed a range of damage states, affected by the structural typology and hazard characteristics. Our study reveals that structures may be damaged or destroyed beyond the lava flow margin, due to thermal effects from the lava flow, fire spread, or from exposure to a range of hazards associated with fissure eruptions, such as steam, volcanic gases, or tephra fall. This study provides a major contribution to the currently limited evidence base required to forecast future lava flow impacts and assess risk.

Keywords Lava flows · Damage assessment · Physical vulnerability · Tephra · Gases · Fire · Kīlauea volcano · Lower East Rift Zone

✉ Elinor S. Meredith
  elinorsi001@e.ntu.edu.sg

1   Earth Observatory of Singapore, Singapore, Singapore

2   Asian School of the Environment, Nanyang Technological
    University, Singapore, Singapore

3   GNS Science, Lower Hutt, New Zealand

4   U.S. Geological Survey, Hawaiian Volcano Observatory,
    Hilo, HI, USA

5   U.S. Geological Survey, Volcano Science Center, Alaska,
    USA

Springer

Introduction

Lava flows pose a threat to communities living near active volcanoes because they may destroy structures and land (Kilburn 2015; Harris 2015) and because they are often associated with other primary and secondary hazards such as proximal ballistics, tephra, fires, and corrosive gas emissions. Lava flows typically move slower than other volcanic flows such as pyroclastic density currents (PDCs), and local residents often have time to respond and evacuate prior to impact (Harris 2015). As a result, deaths attributed to lava flows have remained low, at 4% of all recorded fatal volcanic events since 1600 AD (Brown et al. 2017). However, lava flows have caused considerable destruction to residential and urban areas, such as 80% of Ako village in 1983 (eruption of Miyakejima, Japan: Aramaki et al. 1986), 75% of Chã das Caldeiras villages in 2014–2015 (eruption of Fogo, Cape Verde: Jenkins et al. 2017), and 13% of the city of Goma in 2002 (eruption of Nyiragongo, Democratic Republic of Congo: Baxter et al. 2002), amongst others (Table 1). Lava flows can inundate tens of square kilometres and can reach thicknesses of hundreds of metres during an eruption, with the buried land potentially unrecoverable for decades (Kilburn 2015). Typically, if a community chooses to re-inhabit the area, they may remove the lava itself (the 1973 lava flows of Eldfell volcano, Iceland: Williams and Moore 1983; Morgan 2000) or rebuild structures on top of the solidified lava, once it has cooled enough (the rebuilding of Kalapana Gardens, Hawai'i: Thompson 2018).

Critical to understanding lava flow impacts is the assessment of damage during past events. Ordinal damage states are a widely applied component of efforts to assess impacts from natural hazards, including earthquakes (e.g., ATC 1985; Kircher et al. 1997; Lallemant et al. 2015), hurricanes (e.g., Friedland and Levitan 2009; Tomiczek et al. 2017; Nofal et al. 2021), and tsunami (e.g., Peiris 2006; Ruangrassamee et al. 2006; Charvet et al. 2015). Damage states applied to assets are ordinal scales of damage severity from undamaged to total destruction, determined using observational post-event damage information (Blong 2003a). Descriptions are deliberately generic so that they can be applied to multiple different events and structural typologies, allowing for comparison of damage between and across events (Blong 2003a). By coupling the damage states with the known or inferred hazard intensities at the time of impact, quantitative empirical relationships can be developed that can then be used to forecast potential future damage through the development of vulnerability models (Douglas 2007). Therefore, damage states are an important element of risk assessment and mitigation.

Damage states have been used to categorise volcanic hazard impacts from tephra fall (Spence et al. 1996; Blong 2003b; Hayes et al. 2019; Williams et al. 2020), lahars (Jenkins et al. 2015), and PDCs (Baxter et al. 2005; Jenkins et al. 2013). For a review of volcanic damage states, see Wilson et al. (2014). There are relatively fewer studies assessing lava flow damage, with only one study directly relating lava flow characteristics and damage at the individual building scale (Jenkins et al. 2017). Most studies report lava flow damage as a percentage of urban area or number of buildings destroyed (e.g., Macdonald and Eaton 1964; Williams and Moore 1983; Baxter et al. 2002) or information on the impacts is qualitative (e.g., Isshiki 1964; Nolan 1972; Bonaccorso et al. 2016). This assessment approach limits the empirical evidence available to quantitatively assess lava flow impacts and risk.

Lava flow vulnerability models commonly assume that exposure of a structure to lava results in complete destruction (Jenkins et al. 2014, 2017; Wilson et al. 2014). This assumption contrasts with other hazards such as tephra fall, where damage is seen to vary as a function of hazard intensity (Hayes et al. 2019). However, past accounts of damage associated with lava flows suggest that different degrees of damage will occur depending on the hazard characteristics (e.g., static or dynamic pressure, intensity, temperature), damage mechanisms (direct impact or ignition from fires), and/or structural properties (building materials). For example, the type and thickness of lava on initial contact have been proposed as important determining factors for damage, with thick 'a'ā and block flows more damaging than thin pāhoehoe flows (Blong 1984; Harris 2015; Jenkins et al. 2017). The orientation, shape, and material of the structures have also been found to be important factors to consider with regard to structural resistance to lava flows (Blong 1984; Harris 2015; Jenkins et al. 2017). For example, lava-induced fire appears to be less of a hazard where exposed structures are constructed from masonry or concrete (Vesuvius, Italy, 1906: Blong 1984; Fogo, Cape Verde, 2014–2015: Jenkins et al. 2017). Damage may also extend to buried infrastructure (Tsang et al. 2020) or beyond the flow margin, such as from gases (e.g., Miyakejima, Japan, 2000: "Living with Volcanoes" 2008; Piton de la Fournaise, Réunion Island, 2007: Staudacher et al. 2016; Mount Cameroon, Cameroon, 1999: Wantim et al. 2018) or secondary fire outbreaks from ejected material (Eldfell, Iceland, 1973: Williams and Moore 1983; Kīlauea, Hawai'i, 1960: Blong 1984). Lava flows may also trigger fire spread beyond the flow margin (e.g., Kīlauea, Hawai'i, 2002: McDaniel et al. 2008; Etna, Italy, 2002–2003: Bonaccorso et al. 2016; Pacaya, Guatemala, 2021: GVP, 2021b). Thus, vulnerability models that assume exposed assets experience binary damage from lava flows may not represent the range of damage observed and may limit the ability to accurately forecast damage.

Table 1 Records of lava flow damage to structures from eruptions that damaged houses from 1970 to 2022

Volcano	Date	Damage description	Source
Eldfell, Iceland	1973–1974	~300 houses, fish-freezing plants, and power generating facility destroyed in Vestmannaeyjar	a, b, c, d, e
Etna, Italy	1981	Buildings destroyed, railway line, and 3 major roads inundated	b, e, f
	1983	> 100 buildings destroyed and major road inundated	b, e, g
	2001	Tourist infrastructure and a few houses destroyed, and a highway inundated	e, h
	2002–2003	Damage to Piano Provenzana, tourist infrastructure destroyed, 2 buildings at Rifugio Sapienza destroyed, a major road inundated	e, h, i, j
Fogo, Cape Verde	1995	90% of the main villages, Portela and Bangeira destroyed and main road inundated	d, e, k
	2014–2015	170 buildings destroyed and 90 buildings damaged (75% of Chã das Caldeiras villages), main road inundated, well head covered	d, e
Karangetang, Indonesia	1976	24 houses destroyed, 44 in the path of the flow dismantled	b, d, l
Karthala, Comoros	1977	293 houses destroyed and 566 m of roads inundated	e, m, n, o, p
Kīlauea, USA	1986 and 1990–1991	181 buildings destroyed, the majority in Kalapana Gardens and >10 km of highway inundated	c, d, e, q
	2018	~700 homes destroyed in the Puna District, major roads inundated	e, r, and this study
La Palma, Spain	2021	2988 destroyed and 138 possibly damaged	s
Miyakejima, Japan	1983	~400 buildings destroyed; 80% of Ako village	e, t
Nyiragongo, Democratic Republic of Congo	1977	~400 buildings destroyed in two villages	b, c, d, e, u
	2002	~4500 buildings destroyed; 13% of Goma city	c, d, e, v
	2021	~3600 buildings destroyed	w
Pacaya, Guatemala	2010	3 structures burned	x
	2021	Buildings destroyed	y
Piton de la Fournaise, La Réunion	1977	33 houses and a church destroyed	b, c, d, e, z
	1986–1989	8 houses destroyed and highway inundated	d, e

[a]Williams and Moore *(*1983); [b]Blong (1984); [c]Harris (2015); [d]Jenkins et al. (2017); [e]Tsang and Lindsay (2020); [f]GVP (1981); [g]GVP (1983); [h]Barberi et al. (2003); [i]Bonaccorso et al. (2016); [j]Andronico et al. (2005); [k]Komorowski et al. (2016); [l]GVP (1976); [m]Krafft (1982); [n]Bachèlery et al. (2016); [o]Morin and Lavigne (2009); [p]Mossoux et al. (2019); [q]GVP (1992); [r]Neal et al. (2019); [s]Copernicus (2021); [t]Aramaki et al. (1986); [u]GVP (1977a); [v]Baxter et al. (2002); [w]GVP (2021a); [x]Wardman et al. (2012); [y]GVP (2021b); [z]GVP (1977b)

To investigate the factors that control the degree of damage from effusive eruptions, we carried out remote and field damage assessments of lower Puna, on the Island of Hawai'i, USA, which was impacted by lava flows of the 2018 lower East Rift Zone (LERZ) eruption of Kīlauea volcano. The data collected in this study contribute the most comprehensive available dataset of lava flow damage to date, greatly expanding the limited evidence base for documented lava flow damage. To complement damage surveys for other volcanic hazards, and to provide a reproducible and objective method for evaluating damage severity as a function of hazard intensity, we developed and applied lava flow damage states that categorise damage data collected from aerial and ground imagery and ground-based damage surveys.

First, we describe past lava flow events at Kīlauea volcano and describe our case study area and eruption: the 2018 LERZ lava flows. Next, we present our methods for evaluating the location and typology of pre-event structures, our post-eruption ground-based and remote surveys, and our lava flow damage states and describe how the methods were applied to the case study. Then, we present our results from case study analysis, discussing the correlation between damage and hazard, as well as other key findings.

Lava flow hazards and exposure in the lower East Rift Zone

The Puna District

The vast majority of impacts from Kīlauea lava flows over the past 50 years, including the 2018 LERZ lava flows, have been located within the Puna District on the eastern flanks of Kīlauea volcano on the Island of Hawai'i (Fig. 1).
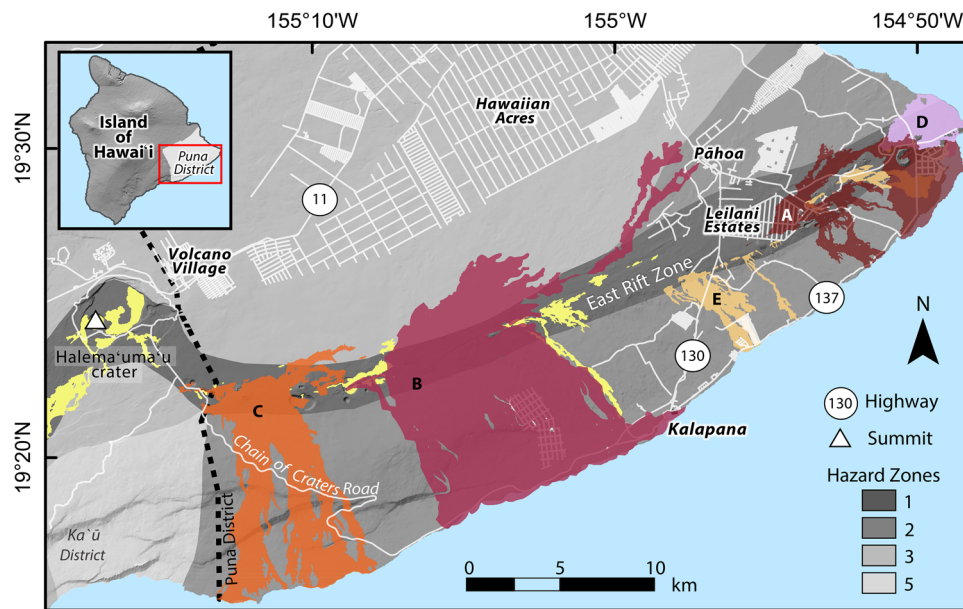
Fig. 1 A map of post-1950 lava flows that have erupted along the East Rift Zone (ERZ) in the Puna District, Island of Hawai'i, with destructive flows highlighted: **a** 2018 lower East Rift Zone (LERZ) lava flows (dark brown), **b** 1983–2018 Pu'u'ō'ō-Kūpaianaha lava flows (burgundy), **c** 1969–1974 Maunaulu lava flows (orange), **d** 1960 Kapoho lava flows (light purple), and **e** 1955 lava flows (light brown). Other flows since 1950 are coloured yellow. Highways, residential roads, hazard zones (zone 4 not within this area), and the Halema'uma'u vent within Kīlauea caldera are shown for context, with the inset showing the location of the Puna District (adapted from Patrick et al. 2020a)

Until 2018, the Puna District had the fastest population growth rate on the Island of Hawai'i (County of Hawai'i 2008), with a population of 35,248 in 2017 as estimated from Landscan data (Rose et al. 2018). Of those residents impacted by the 2018 LERZ lava flows, 24% were below the poverty line (Kim et al. 2019). The 2018 LERZ lava flows originated from a series of fissure vents in and near the Leilani Estates subdivision, located in the east of the Puna District, known as lower Puna (Fig. 1). Lower Puna has a number of important assets such as the Puna Geothermal Venture (PGV) energy plant, supplying 31% of the island with electricity in 2017 (Hawaii State Energy Office 2018); quarries; and tourist hubs of Pohoiki beach and Lava Tree State Park (Fig. 3; Ludwig et al. 2019). The Wai'ōpae Tidepools at Kapoho Bay were destroyed by the 2018 LERZ lava flows (Fig. 3).

In the 1960s, property parcels were built and sold as part of neighbourhoods known locally as subdivisions, containing residential homes, holiday rentals, and other community buildings (County of Hawai'i 2021). However, the subdivisions have low occupancy; for example, within Leilani Estates (Fig. 1), only 37% of the property parcels were occupied before the eruption and were home to ~1600 people, as calculated from a map compiled and given to E. Meredith by the Leilani Community Association (Leilani Community Association, written communication, Dec 2019).

Outside of the subdivisions in lower Puna, property parcels of up to ~1300 acres (~5.3 km^2) are primarily for agricultural, industrial, and residential use, containing a range of structures including large metal or plastic structures (Fig. 2b). Within subdivisions, residential structures are typically one-story timber-frame dwellings with timber walls and predominantly metal sheet roofs (Fig. 2a; Mactagone 2019). Dwellings often have associated accessory buildings, such as arched metal garages or wooden sheds, as well as 4-foot-high (1.2 m) cylindrical metal water tanks with plastic coverings (County of Hawai'i 2021). Most residents rely on catchment systems for water supply, are not connected to a central power supply (Ludwig et al. 2019), and, prior to the eruption, a large proportion of residents were "without adequate housing" (County of Hawai'i 2008, p.38).

Many of the residents have developed a cultural acceptance of living in an area threatened by volcanic activity (Gregg 2005). The island has been designated into nine lava flow hazard zones across the island's five volcanoes, based on where and when past lava flows have occurred, topography, and proximity to vents (Wright et al. 1992). The zones reflect the relative hazard severity, with zone nine as the lowest severity at Kohala volcano, which last erupted over 60,000 years ago, and zone one as the highest severity at the summit and rift zones at Kīlauea and Mauna Loa volcanoes, where vents can open and lava
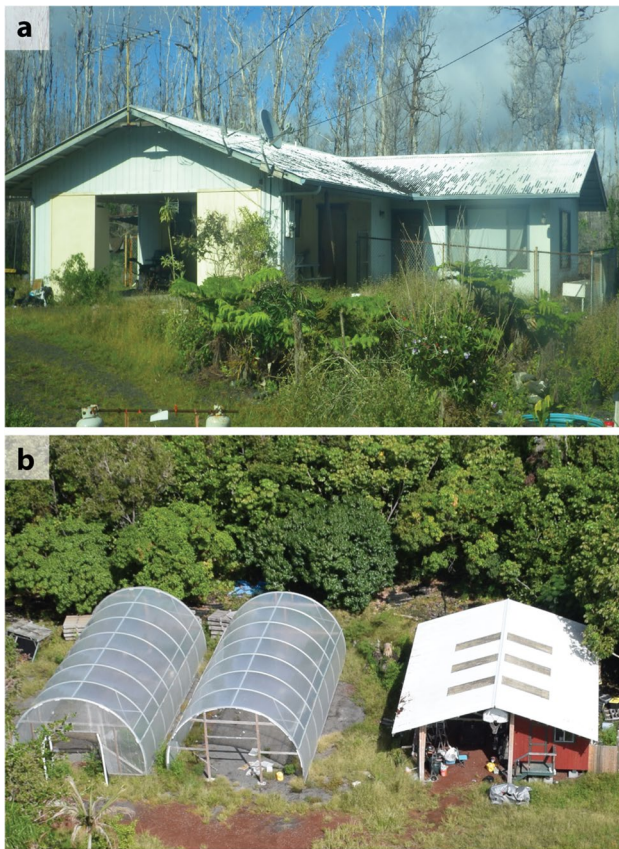
Fig. 2 Photographs taken in lower Puna of **a** a wooden dwelling with a metal roof (taken 18 December 2019) (Photo credit: E. Meredith); **b** non-residential structures: plastic shade houses on the left, wooden accessory building on the right (taken 6 November 2018) (Photo credit: US Geological Survey)

flows have repeatedly resurfaced land in historical time (Fig. 1; Wright et al. 1992). Hazard zones two and three are downslope of zone one and have been frequently resurfaced by lava. The Puna District is predominantly within hazard zones one, two, and three, underlain by lava flows dominantly younger than 500 years BP from the Kīlauea summit, the Kīlauea East Rift Zone (ERZ), and Mauna Loa volcano (Fig. 1; Wright et al. 1992). Those within lava hazard zone one were uninsured for lava damage (Kim et al. 2019).

Located on the windward side of the island, the Puna District's wet climate is typically considered to contribute to a low fire risk (Dolling et al. 2005), with the Hawai'i Wildfire Management Organisation (HWMO) (2013) rating overall fire risk in the district's subdivisions of Leilani Estates and Kapoho as low and high, respectively. However, the environment and buildings are rated as moderate to high fire risk, primarily due to factors such as high-speed prevailing winds and utilities above ground (HWMO, 2013). The frequency of fires has increased in Hawai'i since the

1960s, triggered by humans, either intentionally or inadvertently, volcanic activity, and/or lightning (Smith and Tunison 1992). For example, in 2002, lava-induced fires burned ~13.6 km^2 of land in the Hawai'i Volcanoes National Park (HAVO) (McDaniel et al. 2008), and in 1955, lava-induced fires burned ~5 km^2 of land in the Puna District (Table 2).

Kīlauea volcano and eruption history

Kīlauea is one of the world's most active volcanoes (Macdonald et al. 1983; Tilling et al. 2010). A magma reservoir complex is situated beneath the summit caldera, with magma sometimes supplied along lateral conduits to vents on the rift zones (ERZ and Southwest Rift Zone) (Neal et al. 2019). Since 1800, eruptions were dominantly effusive and characterised by Hawaiian style activity at the summit and along the rift zones, with lava fountains and lava flows, and dominantly explosive periods before 1800, of phreatic and phreatomagmatic activity at the summit (Swanson et al. 2014). Eruptions pose a threat to the local communities: lava flow events since 1950 have damaged infrastructure, roads, and communities along the ERZ (Fig. 1; Table 2) or have stalled close to communities and prompted evacuations, such as the 2014–2015 Puna crisis (Brantley et al. 2019) or the 1977 Kīlauea eruption (Moore et al. 1980). Tephra fall and gas emissions threaten at longer distances, reaching communities outside of the Puna District during the 1983–2018 activity (Longo et al. 2005; Whitty et al. 2020).

For the decade prior to the 2018 LERZ eruption, the Halema'uma'u vent lava lake at the summit was present concurrently with the eruption at the Pu'u'ō'ō volcanic cone located along the ERZ, 20 km from the summit (Patrick et al. 2021). The coupled lava lake level fluctuations at the summit and at the Pu'u'ō'ō volcanic cone suggest that the magmatic system was hydraulically connected (Patrick et al. 2019).

The 2018 Kīlauea eruption

During March and April 2018, inflation around the Pu'u'ō'ō vent and the rise of Halema'uma'u lava lake indicated an increase of pressure within the magmatic system beneath Kīlauea (Neal et al. 2019). On 30 April, the Pu'u'ō'ō crater floor collapsed and magma propagated eastward downrift into the LERZ at ~3-km depth over the subsequent few days (Neal et al. 2019). On 1 May, the Hawaiian Volcano Observatory (HVO) issued a warning of a possible eruption (Neal et al. 2019). At approximately 5 pm HST on 3 May, the first eruptive fissures opened ~20 km east of the Pu'u'ō'ō vent, within the Leilani Estates subdivision, erupting lava (US Geological Survey

Table 2 Recorded impacts to structures and infrastructure from Kīlauea lava flow events since 1950 shown in Fig. 1

| Date	Eruption description	Impact description	Reference
1955	Lava fountains from fissures along the LERZ erupting lava flows through three phases of activity	*Land*: 3900 acres (15.78 km^2) inundated, 1230 acres (4.98 km^2) burned *Homes*: 17 destroyed, 4 uninhabitable, and 3 moved *Roads*: 6.3 miles (10.1 km) of public roads inundated	a, b, c
1960	Lava fountains from fissures along the LERZ erupted 'a'ā lava flows. Efforts to divert the lava with barriers	*Land*: 5.6 km^2 inundated *Homes*: Most of Kapoho (70 structures) and Koa'e destroyed	b, c, d, f, g
1969–1974	Lava flows from Maunaulu vent	*Land:* ~44 km^2 inundated *Roads:* Chain of Craters road inundated	d, f, g
1983–2018	61 episodes of activity of lava fountains and flows from vents along the ERZ. Pu'u'ō'ō vent lava fountains rose to 1500 feet (~450 m)	*Land*: ~144 km^2 inundated, ~13.6 km^2 of land burned in 2002 *Homes*: 215 structures destroyed, including most of Kalapana and Royal Gardens *Roads*: 14.3 km of highways inundated *Other impacts*: Kaimu black sand beach and the Waha'ula Visitor Centre in HAVO destroyed	b, c, d, g, h, i, j
	27th June lava flow in 2014–2015 from the Pu'u'ō'ō vent flowed into and out of cracks in the ground	*Homes*: 1 destroyed, 1 partially inundated *Other impacts*: Roads inundated, cemetery inundated, and utility pole destroyed. Threatened Pāhoa causing widespread disruption, stalling ~150 m from the main village road	c, k, l
2018	Lava flows erupted from 24 eruptive fissures along the LERZ. Effusion rates of ~7 to 100 m^3/s from early to late May and peaking at ~350 m^3/s in mid-June	*Land:* 32.4 km^2 inundated *Homes:* ~700 destroyed including all of Vacationland Hawaii, Kapoho Beach Lots, Kapoho Farm Lots and parts of Leilani Estates and Lanipuna Gardens *Roads:* ~50 km of road network, including parts of Highway 137 and Highway 132 inundated *Other impacts:* ~900 utility poles and 14.5 miles (~23 km) of underground waterlines destroyed	b, c, m, n, o, p, q, r, and this study

[a]Macdonald and Eaton (1964); [b]US Geological Survey (2020a); [c]Tsang and Lindsay (2020); [d]Tilling et al. (2010); [e]Macdonald (1962); [f]US Geological Survey (2013); [g]Babb et al. (2011); [h]Hon et al. (1994); [i]McDaniel et al. (2008); [j]Jenkins et al. (2017); [k]Patrick et al. (2017); [l]Poland et al. (2016); [m]Neal et al. (2019); [n]Kim et al. (2019); [o]Okinaka (2018); [p]Dietterich et al. (2019); [q]County of Hawai'i (2020); [r]Dietterich et al. (2021)

2018; Neal et al. 2019). On 4 May, a M$_w$ 6.9 earthquake, the largest on the island in 43 years, occurred at ~6-km depth beneath Kīlauea's south flank, probably triggered by dyke intrusion (Neal et al. 2019). During the first month of the eruption, a total of 24 eruptive fissures opened up within the LERZ, each up to several hundred metres in length, spanning ~7 km in total (Neal et al. 2019). Fissures were numbered in order of their initial opening, with the most productive fissure 8 later named as Ahu'ailā'au (Office of the Governor 2021).

The first phase of the eruption from 3 to 18 May (weeks 1–2) saw small volume lava flows from relatively short-lived fissures (Fig. 3; Gansecki et al. 2019). From 13 to 25 May (weeks 2–3), the fissure farthest downrift produced fountains, explosive bursts, and relatively viscous flows (Gansecki et al. 2019). The second phase of the eruption from 17 to 27 May (weeks 3–4) saw higher temperature, more mafic lava, with a higher effusion rate (Gansecki et al. 2019). This change in composition from evolved basalt and andesite to hotter mafic basalt indicated a change in magma source from the rift to the Pu'u'ō'ō and Halema'uma'u magma reservoirs (Neal et al. 2019). An increased effusion rate resulted in a channelised lava flow system that advanced southeastward, cut across Highway 137, and reached the ocean on 19 May (Fig. 3; US Geological Survey 2018; Gansecki et al. 2019). The lava flowed into the ocean for another ~10 days (US Geological Survey 2018). In the final phase of the eruption from 28 May to 4 August (weeks 4–14), activity focussed farther uprift, at Ahu'ailā'au, with lava fountains of < 80-m height (Neal et al. 2019) and an effusion rate that peaked at ~350 m^3/s in mid-June (Dietterich et al. 2021). High temperature mafic lava from Ahu'ailā'au formed a channel of pāhoehoe lava that travelled northeastward towards Kapoho (Fig. 3; Gansecki et al. 2019), with measurements of channel surface velocities of up to ~17 m/s (Dietterich et al. 2021). Ahu'ailā'au's channelised lava flow cut across Highway 132 and flowed eastward at Kapoho inundating Kapoho Farm Lots (Figs. 3 and 4). The medial section of the flow consists of braided channels of transitional pāhoehoe-'a'ā lava (Fig. 3; Patrick et al. 2018). The flow reached the ocean at

Fig. 3 The inundation extent of the 2018 lower East Rift Zone (LERZ) lava flows, coloured by week from eruption onset (adapted from Neal et al. 2019). Other post-1950 lava flows coloured in tan. Kapoho Crater, the tidepools, the Lava Tree State Park, and the Puna Geothermal Venture (PGV) are labelled. The most productive fissure: Ahuʻailāʻau (fissure 8) is labelled, along with the associated tephra 1-cm and 0.1-cm isopachs. The flows covered 32.4 km². Helicopter photographs taken after the flow (taken 29 August 2019) show: **a** the proximal section of the flow with the fissures and pāhoehoe lava within Leilani Estates and Ahuʻailāʻau in the centre, facing northwest, **b** the southern ʻaʻā flows over vegetation, facing northeast, and **c** the distal section of the flow with a broad fan of ʻaʻā lava at the ocean entry facing south (Photos credit: US Geological Survey)
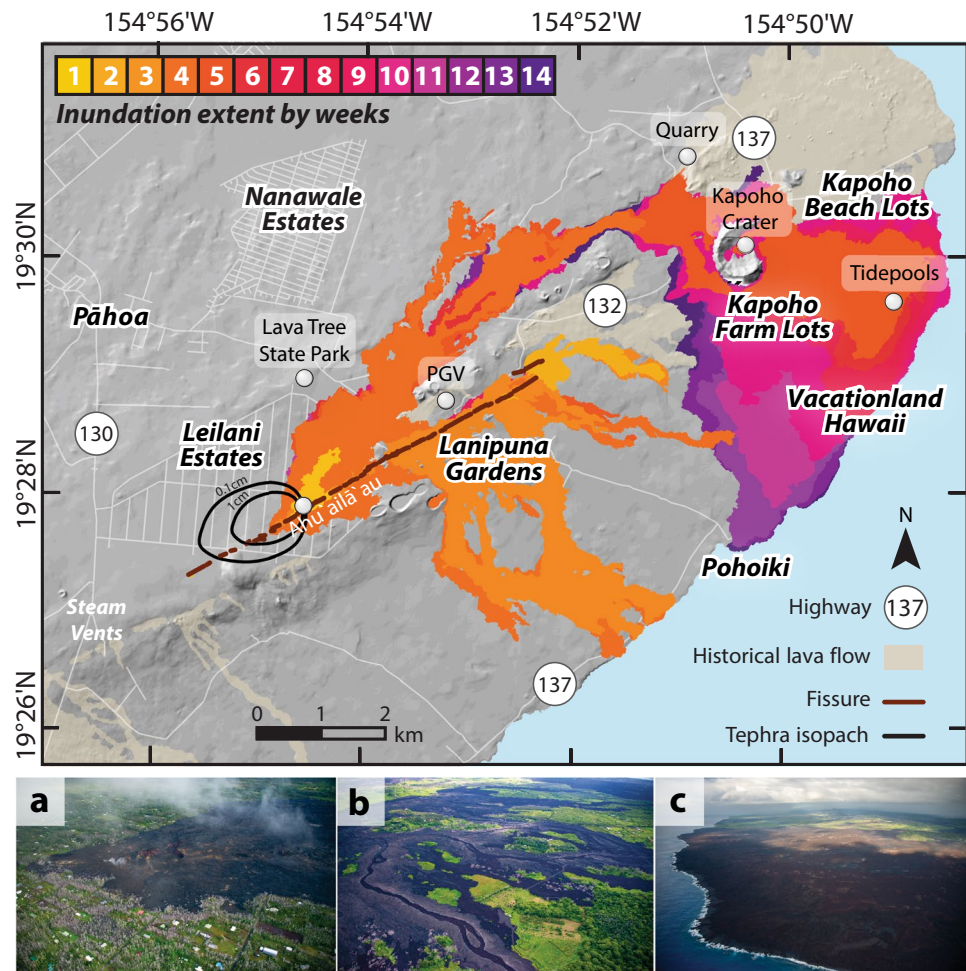
Kapoho Bay on 3 June (week 5) inundating the Waiʻōpae Tidepools (Fig. 3; US Geological Survey 2018). The lava flowed into the ocean for a further two months, widened as a broad fan of ʻaʻā lava (Fig. 3c; Patrick et al. 2018, 2020b). Thinner lateral breakout flows, known as ooze-outs, at the flow margins inundated Kapoho Beach Lots and Vacationland Hawaii (Figs. 3 and 4; Patrick et al. 2018, 2020c). There was an estimated total of 0.9–1.4 km³ of lava (Dietterich et al. 2021), of which Ahuʻailāʻau produced ~92–96% of the total volume (Gansecki et al. 2019).

Days after the collapse of the Puʻuʻōʻō crater, the summit magma reservoir started to deflate along with the lava lake descent and associated daily earthquakes (Patrick et al. 2020b). Widening of the Halemaʻumaʻu crater in the first few weeks of the eruption produced explosions, and on 16 May the first caldera collapse event occurred. The wider caldera collapse events exhibited up to ~2-km-high plumes of ash and associated M_w 5 earthquakes (US Geological Survey 2018; Neal et al. 2019). The final collapse event at the summit occurred on 2 August, and major lava effusion at the LERZ fissures ended by 4 August (Neal et al. 2019).

Reported impacts

Lava flows from the eruption inundated 32.4 km² of land (Fig. 3; Neal et al. 2019). In addition to the impacts to structures and infrastructure listed in Table 2, the lava flows destroyed natural and cultural resources including 3.47 km² of agricultural land, 500 acres (~2 km²) of forest reserves, 80 anchialine pools, the Waiʻōpae Tidepools at Kapoho Bay and Ka Wai a Pele (Green Lake) (Fig. 3; County of Hawaiʻi 2020). It created new beaches and thermal ponds at Pohoiki Bay and added ~3.6 km² of new land (Neal et al. 2019). An estimated 5563 people were directly affected (i.e., displaced permanently or temporarily), of whom 48% (2668 people) were evacuated under mandatory evacuation orders (County of Hawaiʻi 2018; Kim et al. 2019). Evacuation orders and resident access restrictions in place during the course of the eruption were rescinded on 10 September 2018 (County of Hawaiʻi 2018; Civil Defense 2018).

During the eruption, power was disconnected by Hawaiian Electric Light Company (HELCO) from the areas at risk of lava flow impact (Big Island Now 2018). The destruction of ~900 utility poles cut off regions from access to power,

Fig. 4 The cumulative number of buildings in contact with lava (black line) and the cumulative area lava (km2) (purple line), across the weeks of lava effusion. The green background on the left indicates the weeks of predominantly channel emplacement; the blue background on the right indicates the weeks of breakout flows and overflows. By the end of the fourth week of lava effusion, 50% ($n = 894$) of the total number of buildings in contact with the lava were impacted. Below the plot indicates the weeks of most destruction for each of the main residential subdivisions
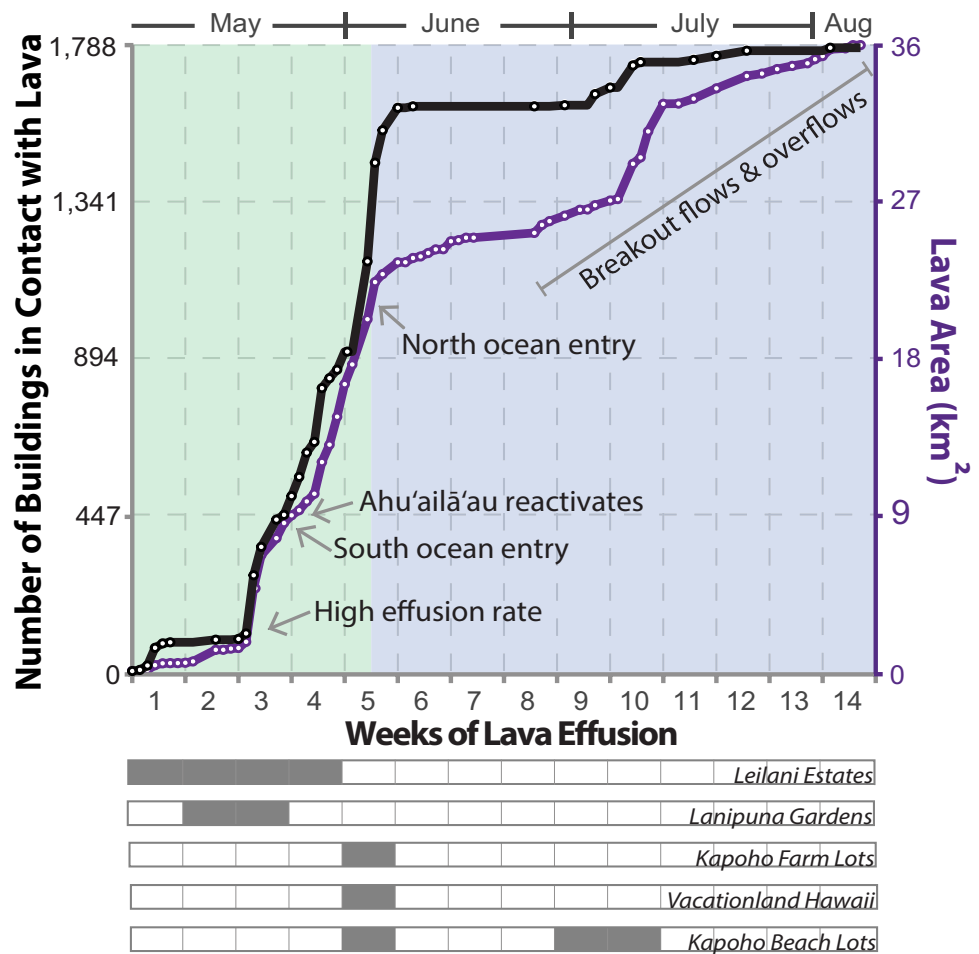
and this was restored to isolated homes months after the end of the eruption (Okinaka 2018). The PGV energy plant was closed shortly after the eruption started, and measures were taken to reduce the risk of toxic gas release if the lava entered the facility (The Guardian 2018). Lava covered two wells of the facility (The Guardian 2018), but there was no reduction in power supply on the island, as alternative sources of energy were used to supplement the electricity service until the power plant re-opened in November 2020 (HELCO 2020).

The LERZ fissure eruption presented other hazards in addition to lava, such as ballistics, gases, and earthquakes. A lava bomb reportedly ejected 200 yards (~180 m) from a fissure, injured one resident who chose not to evacuate (CBS 2018), and 23 tourists were injured on a sight-seeing boat from a lava bomb and smaller ejecta associated with explosions at the ocean entry (Jacobs 2018). The SO_2 emissions that reached a monthly average of ~200 kt/day in June (Kern et al. 2020; Whitty et al. 2020) posed a health hazard to those populations downwind as vog (volcanic smog) (Ludwig et al. 2019; County of Hawaiʻi 2020; Whitty et al. 2020). Magma dyke intrusion triggered earthquakes and

cracks across properties and roads in Leilani Estates and adjacent areas (County of Hawaiʻi 2020).

As a result of the concurrent summit eruption, earthquakes and ground subsidence damaged buildings and infrastructure within HAVO and Volcano Village, caused cracks and sinkholes in Crater Rim Drive and park trails, as well as breaks in water and sewer lines (Ludwig et al. 2019; County of Hawaiʻi 2020). Damage and concern about escalating activity from the eruption at the summit led to the relocation of US Geological Survey (US Geological Survey 2020b) scientists to Hilo and the closure of HAVO for 162 days (NPS 2018; Neal et al. 2019; County of Hawaiʻi 2020). Tourism and agriculture sectors were impacted heavily; the County of Hawaiʻi (2020) estimated 2950 jobs lost and a $415 million revenue loss island-wide from May 2018 to April 2019.

Methods

Our data consisted of (1) a pre-event building inventory, (2) damage data collected remotely from imagery, and (3) damage data collected during in-person field visits. We assessed

structures in the LERZ as these were exposed to lava and/or secondary hazards and have not included structures exposed to explosive activity at the summit. We developed a damage state framework to map the damage quantitatively across the impact area in order to identify and analyse any relationships between hazard intensity and damage. Hazard data were sourced from Zoeller et al. (2020) and US Geological Survey (2020b). Our methodology and workflow are summarised in Fig. 5; we discuss each step in the following subsections.

Pre-event structure inventory

We compiled a geospatial inventory of structures before the eruption to characterise structures including the use, material, footprint area, and location (Table 3). The structure footprint area and location were obtained from Open Street Map (OSM 2017), and this was used as the basis of the structure inventory. We then manually updated these data by digitising an additional 1179 structure footprints, by assessing imagery from before the eruption (27 September 2017 1×1 m resolution Digital Globe satellite imagery, USGS aerial photographs taken on 3 May 2018 ($n = 1504$) and Google Maps StreetView where available). To focus our efforts, we constrained the manual digitisation to within 600 m of the lava flow footprint. The 600-m distance was chosen as the upper limit as observations of fire damage to structures were found ~595 m from the flow margin. We compiled information about the structure use, date built, and number of storeys, as well as the roof, floor, and wall materials from the County of Hawai'i (2021) dataset. For structures with missing data, we assumed the same characteristics as those recorded in data available from the County of Hawai'i (2021) by considering the structure's size, shape, and roof colour in imagery (Table 3). If the structure showed signs of damage or deterioration in condition in the pre-event imagery, such as roof discolouration, this was noted in the inventory. In total, there were 3165 structures in our pre-event inventory (see supplementary material).

Collection of post-event data

Imagery and videos

To analyse damage, we compiled imagery from a variety of sources taken during and following the eruption (Table 4). These were primarily USGS photographs and videos taken on helicopter flights and on foot during and after the eruption, or as part of ground-based damage surveys carried out within 16 months of the event ending. We also included image mosaics of the eruption taken by unmanned aerial vehicles (UAVs), provided by the University of Hawai'i at Hilo (UHH). Images that focussed on infrastructure ($n = 866$) were qualitatively assessed but not included in the quantitative damage assessment, which left a total of 8269 images used in the damage assessment. The majority ($n = 6321$) of images were geo-located, recording the location from where the image was taken. There were 1948 images that were not geo-located, and in these instances we used familiar geographical features, such as the Kapoho Crater, to approximate the locations (Fig. 3). We assigned each photograph to structures in the pre-event inventory if the structure footprint was visible in the image. In total, all structures had at least one and as many as 124 images assigned to them.

Post-eruption ground-based damage surveys

We conducted two ground-based damage surveys in February and December 2019, 6 and 16 months after the end of the eruption. The main goals were to take ground photographs and collect detailed damage data for impacted structures, with a particular focus on structures obscured in aerial imagery. In February 2019, we visited Leilani Estates subdivision and vantage points along the north and south of the lava flow margin. We also visited structures in the area of land surrounded by lava flows, known as a kīpuka, in the south of the flow field. In December 2019, we re-visited Leilani Estates subdivision and structures along Pohoiki

Fig. 5 A conceptual diagram of our approach to the damage assessment, from the development of the structure inventory (purple rounded rectangle), the development and application of damage states (green oval), the development and application of data quality categories (orange hexagon), and finally assessing relationships between the damage and hazard (yellow rectangle)
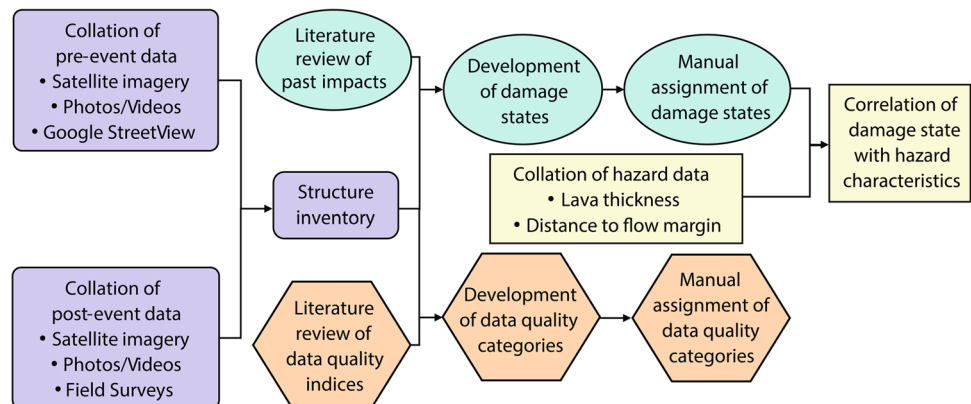
Table 3 Structural use for this study to classify structures by use and material in the pre-event structure inventory, with likely characteristics of each based on building practices in the area

Common characteristics	Dwelling ($n=2038$)	Accessory building ($n=473$)	Water tank ($n=342$)	Farming/industrial ($n=312$)
Shape	Rectangular	Rectangular	Circular	Rectangular
Roof colour	White, green, grey	White, green, grey	Black	White, green, grey, black
Size	~150m²	<120m²	~30m²	>170m²
Material	Wood or metal	Wood or metal	Plastic and metal	Metal and/or plastic

road. Highway 132 had recently reopened, which gave road access to another large kīpuka in the north of the flow field.

We standardised our field-based data collection to ensure consistency across the collected dataset. We did this by creating a survey form for lava flows that standardised damage descriptions using a damage state (see supplementary material). We used Open Data Kit software (Hartung et al. 2010) to be able to collect and store data rapidly on a portable device. The damage survey form was adapted from the ATC-20 Rapid Evaluation Safety Assessment Form for earthquake damage (ATC 2005) to be made suitable for lava flow damage. More specifically, the types of damage were modified to be relevant for thermal-related damage such as charring and melting. The survey allows the user to specify, for each structure, the severity and types of structural damage evident, such as to beams or walls, and non-structural damage evident, such as to windows or cladding. The survey also specifies other geotechnical hazards, which are specific to volcanic hazards, e.g., gas from fissures. The geo-located impact observations and records of associated hazards, along with photographs collected from the field, were assigned to the structures in our inventory. The damage survey form is provided as supplementary material for use in future lava flow assessments.

Data quality framework

We used a variety of data sources in this study that varied in quality and quantity for a given structure, affecting the reliability of the damage state assigned. To account for this variability, we adapted Data Quality (DQ) categories from Hayes et al. (2019) to classify each structure in terms of the data quantity, image acquisition date, and the completeness of the structure or structure footprint shown in the images (Table 5). As it is difficult to determine when deterioration or rebuilding of a structure may take place, it is important to use imagery collected as soon as possible after the eruption ends. We have assigned the classifications for the date of earliest data post-eruption based on the data available for this study (Table 5). The number of images and the completeness of the structure visible in the images also affected the ability to reliably assign a damage state, which have been included in Table 5. The thresholds for each DQ category were defined after all structures and images had been manually evaluated and reflect our qualitative assessment. The data for each structure must meet two out of three criteria to be assigned the DQ category, from least reliable (DQ0) to most reliable (DQ4). For example, a structure that has only satellite images and ground photos (DQ1) showing the total

Table 4 Types of syn-event and post-event visual data used for the damage assessment of structures, including their sources, date taken, and quantity. Duration of videos is up to ~14 min

Imagery	Source	Date	Number
Helicopter photographs	US Geological Survey	Syn-event	875
		Post-event	5533
Ground photographs	US Geological Survey	Syn-event	255
		Post-event	681
	Ground-based surveys	Post-event: February and December 2019	640
Helicopter videos	US Geological Survey	Syn-event	130
		Post-event	12
Ground videos	US Geological Survey	Syn-event	138
		Post-event	1
Satellite imagery	Digital Globe	Post event: 12 May 2019	1
UAV mosaics	University of Hawai'i at Hilo	Syn-event: 18 May 2018, 22 June 2018	2
		Post-event: 9 September 2019	1
		Total:	**8269**

Table 5 Data quality categories used to classify the data used to assess damage to structures. Close-up aerial photos focus solely on one property parcel and wide-angle aerial photos contain multiple property parcels

Category	Description	Criteria (2/3 need to be met or exceeded)		
		Data quantity*	Completeness of structure or structure footprint visible	Date of earliest data post-eruption
DQ0	None	None	None	None
DQ1	Poor	1–2 types	Roof or limited amount of structure visible	> 2 years post-eruption or only syn-eruption
DQ2	Tentative	3 types	< ½ structure visible	1–2 years post-eruption
DQ3	Satisfactory	4 types	> ½ structure visible	1 month–1 year post-eruption
DQ4	Best	> 4 types	All included in photos	< 1 month of eruption

*Data types: Satellite image, wide-angle aerial images, close-up aerial images, UAV images, ground photos, and ground surveys

structure in the imagery (DQ4) and the earliest image was taken 1–2 years post-eruption (DQ2) would be assigned the minimum category met or exceeded by two criteria (DQ1).

Damage state framework

To categorise the damage, we developed a Damage State (DS) schema specifically for lava flows. We aimed to accommodate the range of damage to different components: non-structural elements (DS1) and structural elements (DS2–5), as well as damage severity: from negligible (DS1) to major (DS4) and destruction (DS5) (Table 6). The damage states also record those structures with no visible damage (DS0). Our six-stage schema builds on previous damage states for other volcanic hazards that only consider mechanical damage (e.g., lahar, PDC, tephra fall: Spence et al. 1996; Baxter et al. 2005; Jenkins et al. 2015) by also including thermal damage effects. The descriptions for each of the damage states were compiled after analysis of literature detailing past lava flow damage (Table 1) and from analysis of the 2018 LERZ lava flows imagery collected for this study. For ease of application, the damage states are mutually exclusive but ordinal such that DS3 also includes damage observed at DS2 and DS1. The terminology used in our framework is deliberately generic so that it can be made applicable to any structure type; we have included a schematic of each damage state to support the text descriptions (Table 6).

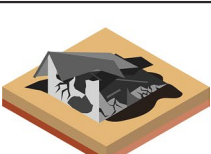## Categorising damage to structures

The damage state was assigned concurrently with the data quality category. Damage states were manually assigned on a structure-by-structure basis by comparing post-event damage data with the pre-event inventory. To retain consistency, this was conducted by one author (EM). If there was no evidence of damage to the structure, the structure was assigned the lowest damage state (DS0). If there was evidence of damage, the damage state descriptions were used to assign a state depending on the severity of damage (Table 6), for example assessing the severity of charred wood or collapse of structural components. Structures that were destroyed were assigned the highest damage state (DS5). Structures shown in imagery as completely buried by the lava flow were assumed destroyed (DS5). We conducted analysis of both structural and non-structural elements, and if there was evidence of multiple damage states, for example minor non-structural melting (DS1) and destruction of a beam (DS4), the most severe of these states was adopted. Any other observations were noted in the database, such as the presence of tephra in the property parcel or cracks in the ground.

Correlating hazard intensity and damage

Due to hazard data availability constraints, we selected the characteristics of lava thickness and proximity to the lava flow as proxy hazard intensity metrics, but we recognise that morphology, viscosity, and velocity may also contribute. The distance from the lava flow and its relevant thickness were calculated using a lava flow shapefile (Zoeller et al. 2020) and the 1×1 m resolution lava flow thickness map (US Geological Survey 2020b), created using pre- and post-eruptive LiDAR data. To compare how damage varies as a function of these characteristics, structures were split into two categories: those in contact with lava and those not in contact with lava. For structures in contact with lava, the thickness of lava was recorded at each of the structures' vertices, and the largest thickness value for each structure was selected and used as a proxy for the hazard intensity to which the structure was exposed. For those structures not in contact with lava, the distance between the lava flow and the structure was used as a proxy for the hazard intensity to

Table 6 Ordinal six-point damage state schema developed for lava flow damage, with descriptions and associated schematic

Damage State	Severity	Description	Schematic
DS0	No visible damage	No evidence of structural or non-structural damage.	
DS1	Negligible	Negligible structural damage, minor surface damage, such as melting of plastic exterior façade.	
DS2	Minor	Minor structural or non-structural damage, such as cracking and holes in wall, or <30% inundated.	
DS3	Moderate	Partial structural damage or roof destruction, partial destruction of non-structural wall, or 30-60% inundated.	
DS4	Major	Major structural and non-structural damage; wall, column, beam or roof collapse, or >60% inundated.	
DS5	Complete destruction	Complete structural destruction or burial.	

which the structure was exposed. For structures in contact with lava, we also measured the distance of structures to the flow margin.

Results and discussion

Below, we summarise and discuss the results of the damage assessment. We interpret the data quality and the damage states assigned by ground-based and remotely sensed data and their relation to selected proxies of hazard intensities, in contact and not in contact with the lava flow. We discuss the importance of factors affecting the impacts, such as building material, accessibility, and functionality. We then investigate the potential use of these findings within risk assessments.

Damage data quality

The large majority of structures (96%; 3044) were assigned a data quality category of "satisfactory" (DQ3) or "best" (DQ4) (Fig. 6). This high data quality was because 83% of the photographs ($n = 6867$) used in the assessment were taken post-eruption and the majority (95%) of structures ($n = 2992$) had the total footprint or structure visible in the imagery. There were 1566 structures (49%) that were clearly seen in the satellite imagery as destroyed by lava flow inundation and assigned DQ3. Structures that were damaged or destroyed (DS1–DS5) and with high data quality categories (DQ3–DQ4) likely had high quality data due to photographers focussing on damaged structures when gathering images on foot. The relatively lower data quality categories (DQ1–DQ2) assigned to 4% of structures ($n = 121$; Fig. 6)
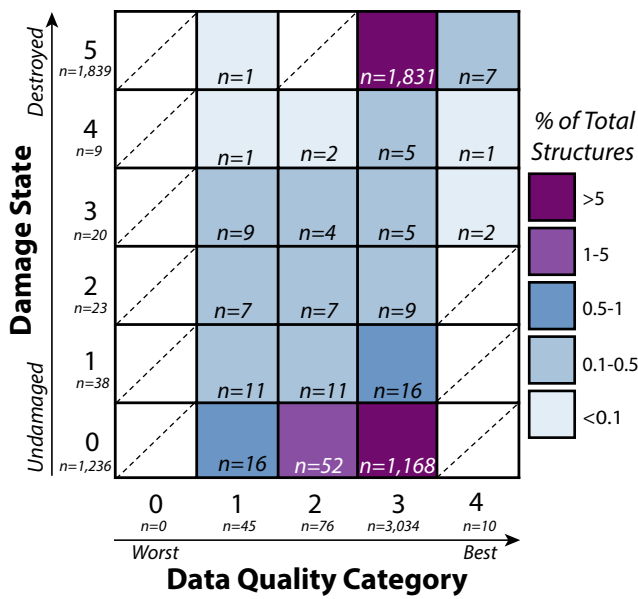
Fig. 6 Each structure within the damage assessment classified by Damage State (DS) and Data Quality (DQ) category. The colour of the boxes reflects the % of structures within that DS-DQ combination, with the number of structures shown in the box (total number of structures = 3165). There are no structures classified as DQ0

were due to either: (1) the images (n = 1389) used in the assessment being taken during the eruption, limiting our ability to reliably assign a final damage state as further damage may have happened after the photograph was taken and/ or (2) less than half of the structure being visible in imagery (n = 61), limiting our ability to assess the total structure.

These lower data quality categories (DQ1–2) likely had access challenges, preventing photographers from taking photos on foot. No structures were assigned DQ0 (Fig. 6).

We found it relatively easier to assign structures that were destroyed (DS5), than other damage states, with few images. However, it is important to have higher data quality categories (DQ3–DQ4) for the damaged but not destroyed (DS1–DS4) structures to be able to reduce uncertainty in the assignment of damage states. It is also important to have close-up imagery and ground-surveys of structures that appear undamaged (DS0) as it was difficult to assess minor damage solely from satellite or wide-angle helicopter imagery.

Damage distribution

The number of structures impacted (DS1–DS5) during the LERZ lava flows event (n = 1929) is the highest on record for Kīlauea and one of the highest on record globally for a single effusive eruption. We assessed a total of 3165 structures, with 1839 (58%) destroyed (DS5), 90 (3%) damaged (DS1–DS4), and 1236 (39%) showing no signs of damage (DS0); all DS0 structures were outside the lava flow footprint (Fig. 7). We overlaid the lava flow footprint onto a map of property parcels (County of Hawai'i 2021) and farmland (Office of Planning 2020) to identify the proportions of each impacted by lava flows. Of the property parcels, 631 were completely inundated by lava and 1040 were partially inundated by lava. For farmland, 3.47 km² was buried by lava flows, including 1.47 km² of papaya farms (42% of the destroyed farmland). Lava flows from

Fig. 7 Map showing the 3165 assessed structures with their assigned damage states: DS0 (white dot), DS1 (light orange dot), DS2 (dark orange), DS3 (magenta dot), DS4 (purple dot), and DS5 (dark purple dot). The central kīpuka is outlined in black. The majority of destroyed (DS5) structures are within the flow footprint, with a range of damage states (DS0–DS5) presented at the lava flow margin and farther away from the flow margin
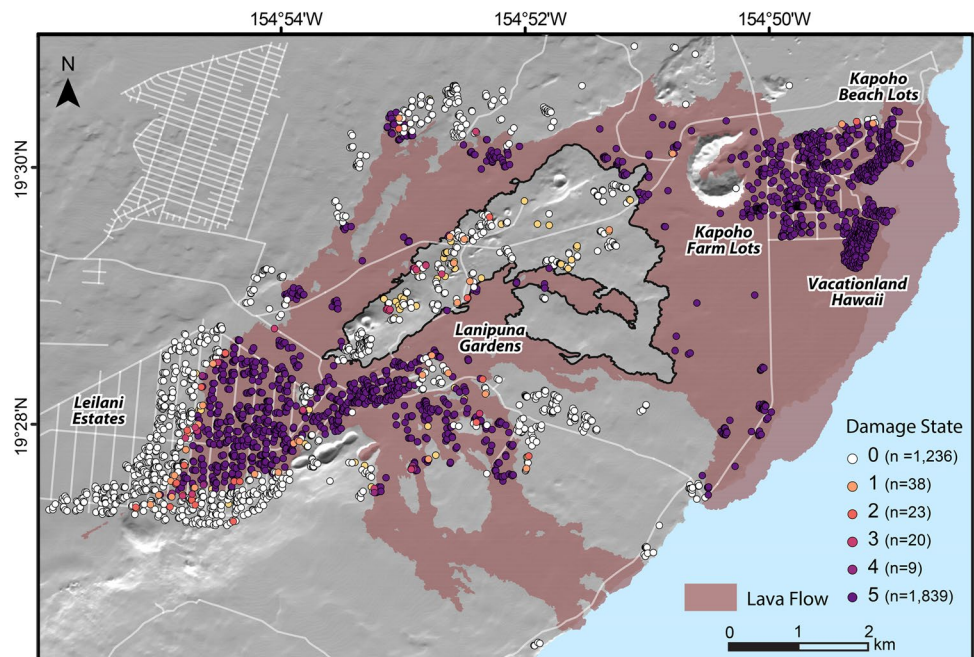
Ahuʻailāʻau (originally fissure 8) destroyed 1.88 km² of farmland (54% of the destroyed farmland). The 2018 LERZ eruption destroyed the entirety of Vacationland Hawaiʻi and Kapoho Farm Lots, large parts of Leilani Estates, as well as the majority of Kapoho Beach Lots, and Lanipuna Gardens (Figs. 3 and 7). Relatively few recent lava flow events have destroyed such a large proportion of multiple communities (75% of two villages in the 2014–2015 eruption of Fogo, Cape Verde: Jenkins et al. 2017).

Damage associated with the 2018 LERZ lava flow event is near binary (Fig. 8), with a range of damage states along the flow margin (Fig. 7). Of the 1929 structures that showed signs of damage or that were destroyed (DS1–DS5), the large majority (n = 1839; 95%) were destroyed (DS5); of these, 1767 were in contact with lava and 72 were not in contact with lava (Fig. 8). However, the remaining structures (5%, n = 90) were classified as damaged but not destroyed (see DS1–DS4 in Fig. 7); of these, 19 were in contact with lava (found up to 17 m from the flow margin), and 71 were not in contact with lava (Fig. 7). This range of damage shown in Fig. 8 contradicts the common assumption that damage from lava flows is binary with contact with lava leading to destruction and no contact with lava leading to no damage.

Damage to structures in direct contact with the lava flow

The large majority of the 1786 structures in contact with the lava flows resulted in high damage states (DS4–DS5: n = 1774; 99%), and structures in contact with > 2-m thickness were all classified as destroyed (DS5: n = 1566; 88%). This destruction points to the vulnerability of these structures to high lateral pressures and temperatures and suggests that the assumption of binary vulnerability holds if the lava flow is > 2 m thick. Within the main flow channels, all

structures were buried or swept away by direct impact with the lava flows (DS5) and there was no evidence of the structures in post-eruption imagery. Of the total structures in contact with the flow, 1206 (68%) were damaged or destroyed within the first 5 weeks of the eruption, when the parent channels were being emplaced (Fig. 4). After the emplacement of the parent channels, ʻaʻā lava destroyed structures as lateral breakout flows at the distal end of the flow. ʻAʻā lava has a greater initial thickness and velocity than pāhoehoe flows (Kilburn 2015). This ʻaʻā lava destroyed structures at Vacationland, Kapoho Farm Lots, and Kapoho Beach Lots (Figs. 3 and 4).

At shallow thicknesses (< 2 m), structures exhibited a range of damage, from DS1–5 (n = 220) (Fig. 9). When overlaying the flow thickness map onto the lava flow chronology map in Fig. 3, the shallow lava (< 2 m) correlates to the southern flows, along the flow margins and also to where there are overflows from the channel of pāhoehoe style lava, after the emplacement of the parent channels (Fig. 10a). Pāhoehoe lava initially is emplaced as thin lobes and inflates to a greater final thickness (Kilburn 2015). Approximately 32% (10.3 km²) of the lava flows are < 2 m thick, predominantly along the flow margins. There were < 2-m overflows that occurred during weeks 6 and 10–11 of the eruption close to the fissures in Leilani Estates, ~1–2 weeks after the parent channel had been established (Fig. 3). They also occurred during the final two weeks (13 and 14) of the eruption, ~8 weeks after the Ahuʻailāʻau lava flow channel had been established, in the north of the lava flow field (Figs. 3 and 10a). The lowest damage (DS1) was only obtained by structures where lava contacted the building at < 0.4 m (Fig. 9). In some cases (n = 36), structures were not totally surrounded by the lava but lava-triggered fires resulted in complete destruction (DS5). In one case, a metal structure of DS3 in contact with the lava flow triggered a fire by heating

Fig. 8 Number of structures of each damage state classified by structure type for structures **a** not in contact with lava and **b** in contact with lava. There were no structures in contact with the lava that remained undamaged (DS0), meaning that all structures in contact with lava sustained some level of damage
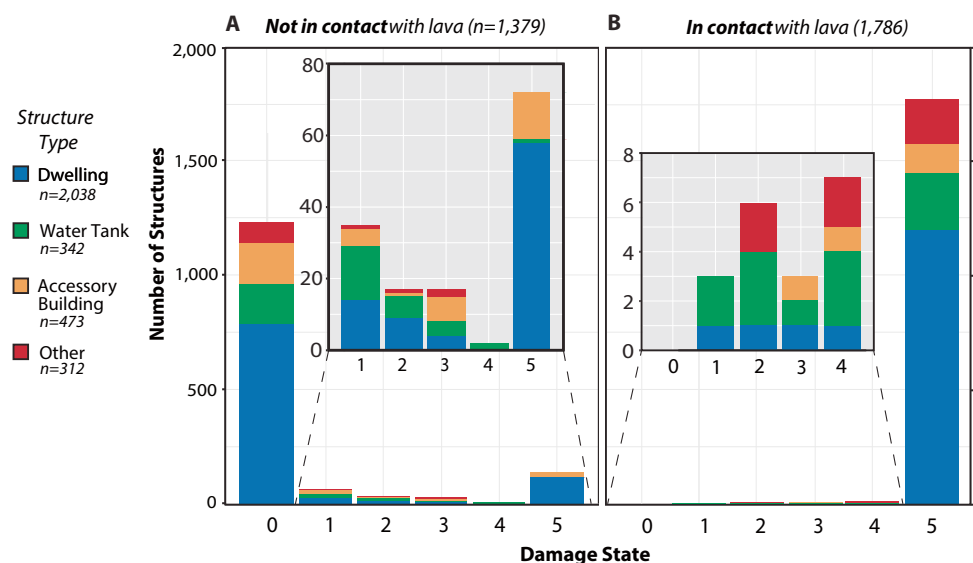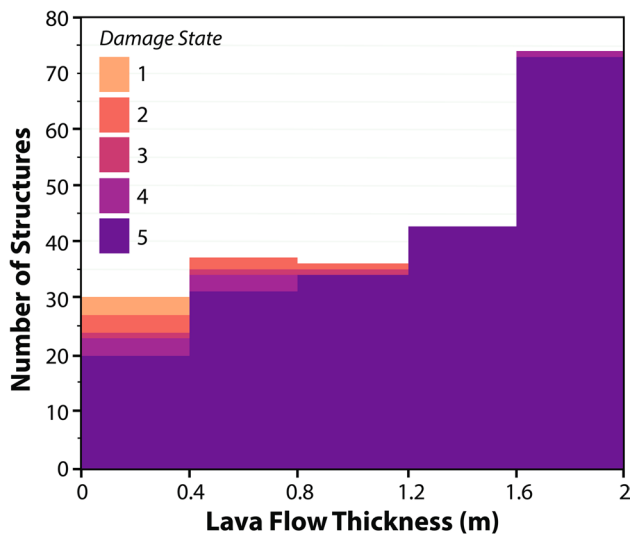
Fig. 9 The number of structures in contact with lava < 2 m thick ($n=220$) categorised by damage state: DS1 ($n=3$), DS2 ($n=6$), DS3 ($n=3$), DS4 ($n=7$), and DS5 ($n=201$). All remaining structures ($n=1565$) in contact with lava flow of > 2-m thickness were destroyed (DS5). No structures in contact with the lava flow were undamaged (DS0)

and subsequent explosion, possibly of a propane tank or vehicle engine (Fig. 10c).

Of total structures in contact with the flow, 580 structures (32%) were damaged or destroyed after the channel reached the ocean on 5 June, when the distal flow region widened by 'a'ā breakout flows or by pāhoehoe overflows (Fig. 4). Lava breakout flows and overflows are inherently difficult to model and are not captured in lava flow forecast models (e.g., Harris and Rowland 2001; Favalli et al. 2005; Del Negro et al. 2005), and so a buffer of potential impact wider than the modelled lava flow channel footprint might be appropriate.

Building characteristics and damage

The damage states appear to be dependent on the structure material and shape. Metal structures demonstrated resistance to direct and indirect lava flow effects whilst structures made from wood or plastic were particularly vulnerable and destroyed (DS5) if in contact with the flows (Fig. 11). For example, of the 18 cylindrical metal water tanks in contact with lava < 2 m thick, 50% ($n=9$) were destroyed (DS5) and 50% ($n=9$) were damaged (DS1–DS4) compared to over

Fig. 10 Photographs taken by helicopter of **a** an aerial view of breakout flows of 'a'ā textures and pāhoehoe overflows from a main Ahu'ailā'au (fissure 8) lava flow channel in the north of the flow field and damaged farming structures (taken 20 May 2018), **b** lava of < 2-m thickness partially surrounds a water tank indicated with a dashed white circle (left), plastic farming structures damaged in contact with lava (centre), and plastic farming structures damaged but not in contact with lava (right) (taken 2 September 2018), and **c** a metal structure in contact with the lava flow, which appears to have suffered fire damage that resulted in the collapse and corrosion of the metal roof classified as DS3 (taken 6 November 2018) (Photos credit: US Geological Survey)
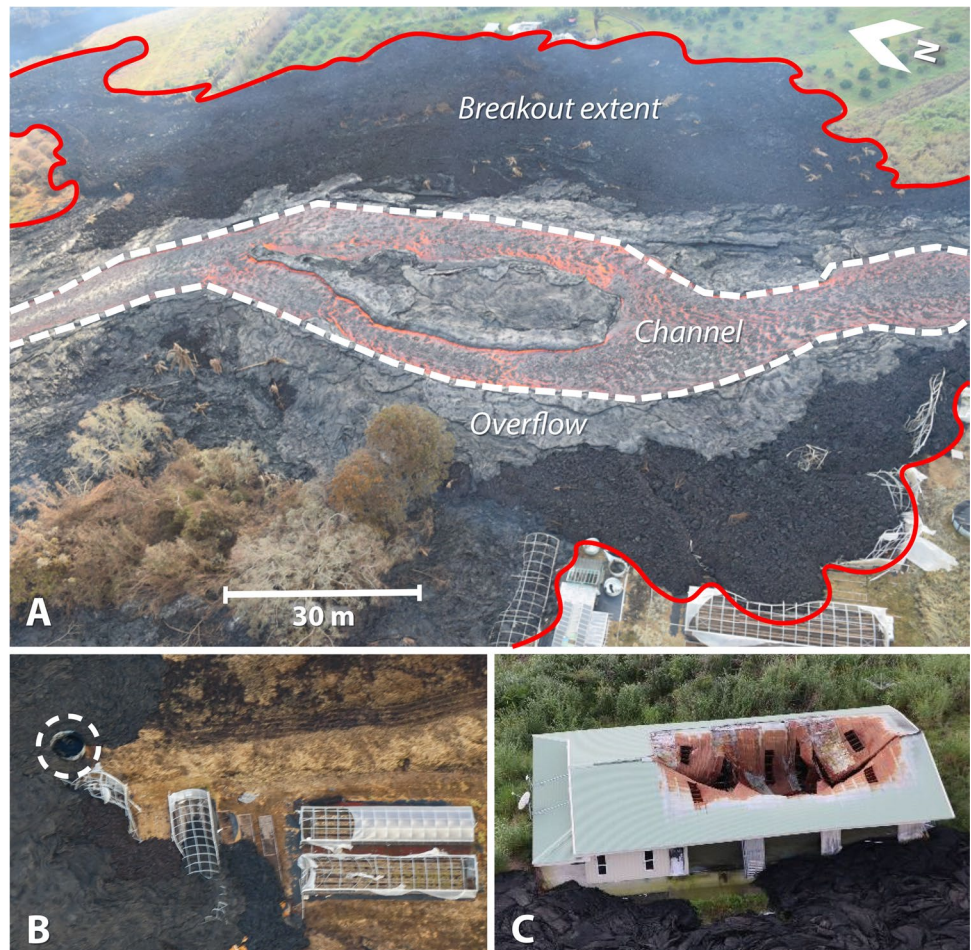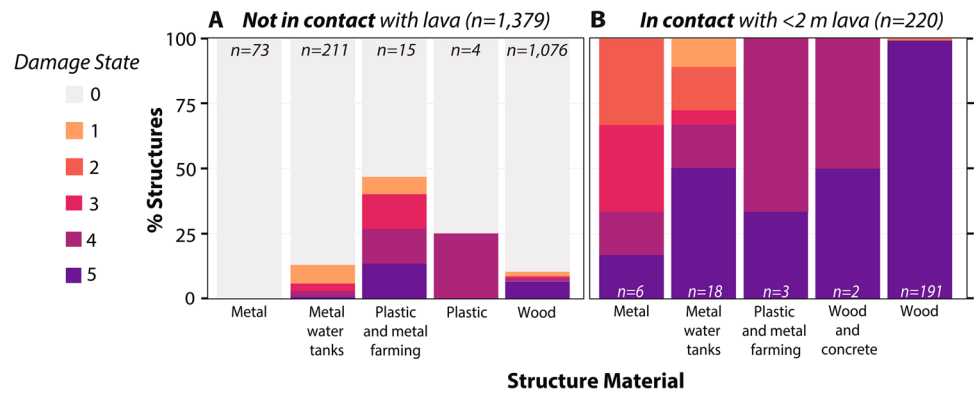
Fig. 11 Percentage of each structure material classified by damage state for structures **a** not in contact with lava and **b** in contact with lava < 2 m thick. All structures in contact with lava > 2 m thick were destroyed (DS5) and not included here, and no structures in contact with lava were undamaged

99% of wooden structures destroyed (DS5) in contact with lava (Fig. 11). Cylindrical masonry buildings during the Fogo lava flows were also resistant to thin flows (Jenkins et al. 2017). Potentially, the resilience of circular structures could be due to the strength of a convex wall placed into compression under the static or dynamic pressure of the lava (Jenkins et al. 2017), information that could be valuable in planning more resistant structures, for example those housing critical infrastructure.

Damage to structures not in direct contact with the lava flow

Of the 1379 structures that were not in direct contact with lava but were within 600 m of the lava flow margin, 10% ($n = 143$) were damaged or destroyed (Fig. 12). Half of the structures that were within 20 m of the lava flow margin were damaged or destroyed (Fig. 12). Thermal effects from the lava and fire, as well as tephra, resulted in a range of damage states, as opposed to complete destruction. For example, 15 structures experienced melting of plastic cladding or covering, but no other damage to the structure (Fig. 13a). Video footage from the eruption showed, in some cases, that wooden structures close to the lava flow did not ignite until the lava was in contact with the structures. This delayed ignition may be due to differing moisture content and wood thickness, which plays a large role in ignitability (Jenkins et al. 2013), or differing lava flow crust thickness that affects the efficiency of thermal conductivity (Blong 1984). As a result, indirect thermal and fire damage extends the range of potential damage from a lava flow beyond the lava flow footprint, but the relationship is not simple (Figs. 12 and 13).

Lava-induced fires were a prevalent cause of damage, with damage to structures up to 595 m from the lava flow margin (Figs. 12 and 13). Fire damage was observed predominantly in the southwest direction away from the lava flow, in the downwind direction of prevailing trade wind; we hypothesise that fire spread due to volcanic gases downwind from the vents, ocean entry, or the flow itself, killing and drying vegetation in this direction (Fig. 13c). Footage also

shows blue flames from ground cracks close to the lava flow margin, likely where heat had triggered methane combustion underground. Blue flames have commonly been observed during lava flows, for example during the 1944 Vesuvius lava flows (Bracker 1944). Fires were extinguished by fire-fighting services during the 2018 LERZ eruption, but the extensive damage in the central kīpuka suggests that without this mitigating action, damage could have been much greater (Fig. 7). The central kīpuka was inaccessible to firefighting services during the eruption, and fires diminished naturally with the lava flows acting as fire breaks. This inaccessibility contrasts with other lava flows at Kīlauea, such as the 1990 Kalapana flow field, where the access of roads was not as restricted (Mattox et al. 1993). Therefore, steps to reduce the fire risk in future eruptions during or prior to evacuation, such as removing propane tanks, vehicles, and easily
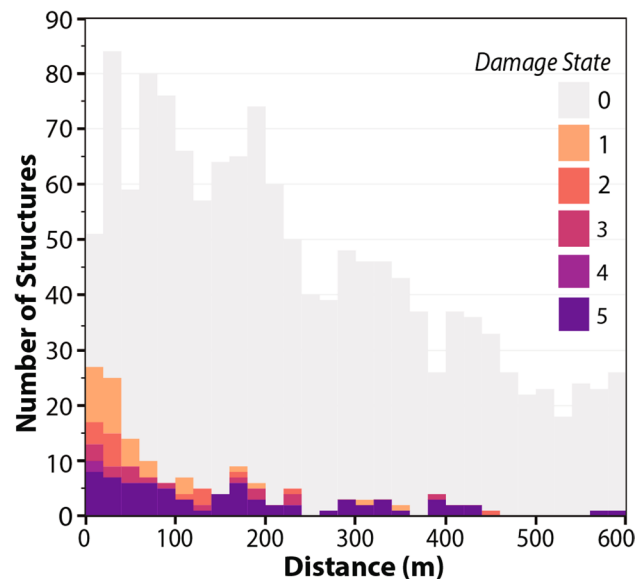

Fig. 12 The number of structures ($n = 1379$) observed at distance (m) from the lava flow margin categorised by damage state: DS0 ($n = 1239$), DS1 ($n = 35$), DS2 ($n = 17$), DS3 ($n = 17$), DS4 ($n = 2$), and DS5 ($n = 72$). Damage was observed up to 595 m from the lava flow

Fig. 13 Photographs taken during the lower East Rift Zone (LERZ) eruption of **a** a wooden dwelling not in contact with the lava flow categorised as DS1, with melting of plastic cladding caused by the thermal effects of the lava (taken 6 November 2018), **b** damage to a structure by fire classified as DS5 (foreground) and a metal water tank categorised as DS1, with melting of plastic covering caused by the thermal effects of fire (background) (taken 6 November 2018), and **c** green vegetation in the north side of the lava flow channel and dried vegetation with fire damage in the south side (taken 29 June 2018) (Photos credit: US Geological Survey)

available combustible materials (outdoor furniture), could reduce the potential for fire damage.

Not all structures were affected by fires, and damage appears sporadic across the southwest direction. This highlights the challenges of forecasting where fire damage will occur during a lava flow event; fire spread is a function of wind speed, wind direction, fuel availability (from vegetation, structures, and infrastructure) and topography (Baxter et al. 2002; Jenkins et al. 2017). Another factor potentially affecting fire spread for the 2018 LERZ eruption is the high humidity of the area, with convective clouds and rain showers that formed over and downwind of the active fissures (Kern et al. 2020). A buffer of potential fire impact up to 600 m around a lava flow footprint would have been sufficient and may provide a preliminary minimum estimate for such a buffer when assessing future lava flow risk, allowing for the potential of lava-induced wildfire damage. Considering the potential for eruption-related fire damage might be particularly important for timber buildings, and in Hawai'i lava flow hazard zone one, where many homes are uninsured for direct lava flow impact but may be covered for fire damage (Kim et al. 2019).

Other observations of impacts and hazards

During the eruption, SO_2 emissions from fissures and flows caused corrosion to structures and damaged vegetation. Corrosion was observed at all metal structures in contact with the lava and at some structures not in contact with lava, in the southwest direction of Ahuʻailāʻau, in the downwind direction of prevailing winds (Fig. 14). These emissions decreased following the end of the lava effusion (Kern et al. 2020; Whitty et al. 2020). When we visited in February and December 2019, we observed emissions of steam from vents, caused by magma interacting with rainwater and groundwater, over a year after the initial eruption had ended,

which likely contributed to the weakening of structures. These hazards and impacts potentially affect the ability for residents to return and live in their homes long after a lava flow event has ended. By the time of our second field visit in December 2019, one resident had dismantled their home as a result of impacts from emissions. Thermal and gas impacts to buildings and infrastructure have also been reported at other volcanic eruptions (e.g., Miyakejima, Japan, 2000: "Living with Volcanoes" 2008; Piton de la Fournaise, Réunion Island, 2007: Staudacher et al. 2016; Mount Cameroon, Cameroon, 1999: Wantim et al. 2018). Tephra associated with minor explosive activity was ejected onto properties in the vicinity of eruptive fissures in Leilani Estates, requiring clean-up by residents (Fig. 14a). We identified eight structures that had been impacted by tephra, with most ($n=6$) classified as DS1 (Fig. 14c). Lava bombs ejected from the fissures reportedly caused human injuries (CBS 2018), and helicopter imagery showed a roof with solar panels damaged from large clasts (Fig. 14c). There were also reports of seismic damage to structures in Volcano Village caused by earthquakes associated with the summit crater collapse (County of Hawai'i 2020). Given these additional impacts, it is clear that a multi-hazard approach is needed to comprehensively assess damage from eruptions, and the provision of such empirical data is useful for anticipating future impacts from these events.

Impacts to accessibility

GIS analysis showed that structures were indirectly impacted by lava flows as they cut access to infrastructure and property parcels (Table 7). The lava flows isolated 24 km^2 of land, and roads could only be reconstructed when the lava flows had sufficiently cooled. For example, Highway 132 reopened ~15 months after the eruption ended, on top of 7-m lava thickness (County of Hawai`i 2019; US Geological

Fig. 14 Photographs taken from helicopters of **a** structures with white roofs covered in tephra, close to a fissure in the foreground; roofs of structures with tephra clean-up evident in the background. Vegetation damaged by gas and steam emitted from the fissures. Ground-surveys showed corrosion to structures from gas and steam impacts (taken 6 November 2018), **b** fissures that have opened underneath a dwelling that is still intact (DS1) (taken 6 August 2018), **c** damage to solar panels (left) and metal roof (right) of a dwelling by large clasts classified as DS1 (taken 6 November 2018), and **d** structures with no access roads, located in a kīpuka surrounded by lava (taken 18 March 2019). Photos credit: US Geological Survey

Survey 2020b). By the time of our first fieldwork in February 2019, Highway 137 was partially rebuilt and had reopened, and by the time of our second fieldwork in December 2019, Highway 132 was rebuilt and had reopened, which gave us access to more structures during the ground-based damage surveys. Cracks across roads still restricted access during our fieldwork and were observed across property parcels and roads in Leilani Estates and across Highway 130, shown in field imagery (Fig. 14b). These restrictions highlighted that

Table 7 Accessibility post-eruption for structures in our study area, not surrounded by the lava flow and the structures' assigned damage states; structures with no access have all roads covered by lava, structures with restricted access have one or more of their access roads covered in lava, and structures with full access have no access roads covered in lava

DS	No access	Restricted access	Full access
0	694	147	395
1	26	4	7
2	14	6	2
3	14	3	3
4	8	0	1
5	91	9	15
Total:	**847**	**169**	**423**

standing structures, which may still be technically habitable with low damage states, could be difficult to access in the eruption aftermath (Fig. 14d). This degree of restriction may delay a community's recovery.

Implications on structure functionality

Lava inundation or fire damage is likely to severely reduce the monetary value of a structure (Blong 1984). For structures that are not directly impacted by the lava, the functionality may be compromised, even for structures that exhibit little to no physical damage, due to damage to critical infrastructure such as water or power, lack of access, fissures opening across properties (Fig. 14b), or tephra requiring clean-up. For example, even minor damage to water tanks, such as corrosion or melting of the plastic covering, as well as water acidification from the ash and/or gas, is likely to make the water unsafe for consumption (WHO 2011; Wilson et al. 2012; Proctor et al. 2020). Despite attempts to protect utility poles during the 2014 lava flows in Pāhoa (Tsang and Lindsay 2020), no such attempts were made during the 2018 LERZ lava flows, and video footage showed destruction of utility poles by fire. Therefore, even structures assigned a lower damage state may be rendered unusable or their functionality affected.

How quickly residents returned to their homes is likely a function of damage, access, availability of utilities, clean-up requirement, public policy, concerns regarding looting, financial situation of the homeowner, and also the attachment of locals to their land. As an anecdotal example, one resident suffered minor damage (DS1) to their home, partial lava inundation to their property parcel, and loss of possessions from looting. These combined factors contributed to the resident not wanting to return home when we spoke with them in December 2019. Whilst the lava flow damage states that we developed only consider physical damage, the development of associated "functionality" states that consider the potential impacts from loss of functionality, dependent on structure use and accessibility, would provide a more holistic representation of lava flow impact.

Conclusions

This work has developed the first non-binary framework for assessing damage to structures from lava flows and applied it to the 2018 lower East Rift Zone (LERZ) lava flows at Kīlauea volcano, Hawai'i. Satellite imagery and photographs taken of this eruption, as well as post-eruption ground-based survey data collected as part of this study, form the largest available impact datasets documenting an effusive eruption. The damage state schema and ground-based damage survey form we created and presented in this study can be applied to assess damage at future lava flow crises or retrospectively applied to past events with sufficient data. This study adds lava flows to the hard-to-reach and/or dangerous zones where field observations of building damage are spotty, non-existent and/or too extensive to assess efficiently from the ground, such as in the cases of hurricanes, conflict, earthquakes, tsunami and wildfire (e.g., Dong and Shan 2013; Witmer 2015; Koshimura et al. 2020).

The LERZ lava flows inundated 32.4 km^2 of lower Puna, destroying 1839 structures and damaging 90 structures, which is one of the highest recorded numbers of impacted structures from a lava flow event. Over half of the total structures damaged or destroyed were impacted by the end of the fourth week (out of 14 weeks in total). After the lava flows reached the ocean, 580 structures (30% of total impacted) were damaged or destroyed by breakout flows or overflows. Through the course of an eruption, structures close to the lava flow channel may not be damaged initially, but are still at risk from later, lateral breakout flows, and overflows widening the flow field. Our study also shows that in a lava flow event, structures may be exposed to a range of secondary and indirect hazards, such as fire spread, tephra fall, ground cracking, thermal stress, and steam/gas emissions.

This study shows that the widely applied assumption of binary damage from lava flows is an oversimplification that limits our ability to accurately forecast future damage associated with effusive eruptions. We found that structures impacted by thicker lava (> 2 m) did abide by the assumption of binary impact (complete destruction). Structures impacted by thinner lava (< 2 m) as overflows or along the flow margin exhibited a range of damage states with circular and metal structures being particularly resilient. We also found that damage occurred beyond the lava flow margin. Thermal and fire damage occurred at structures up to ~595 m from the flow. Fire was a major mode of indirect damage during the 2018 LERZ lava flows. In advance of a lava flow event, a buffer area of potential damage could be applied around the forecast lava flow in order to anticipate impacts beyond the lava flow margin.

We found that the eruption caused impacts to structure functionality beyond the direct damage, such as to road networks, water tanks, or utility poles. The damage state framework developed here could be expanded to consider functionality state as a function of time through the course of the eruptive crisis and during the recovery phase; this approach would provide a more holistic assessment of the impacts and potential losses that would support preparedness and recovery from lava flow events. Accounting for the qualitative social, cultural, and economic factors would also be important, but they are hard to capture within a purely quantitative approach. A holistic approach is therefore needed when preparing for and recovering from lava flow events, considering a range of hazards associated with fissure eruptions.

This study greatly expands the amount of currently available empirical data on impacts associated with lava flow events. The damage states developed in this study can be used to further constrain relationships between the lava flow hazard characteristics and damage severity, providing an evidence base from which forecast models of impacts can be developed. We hope that the data and insights provided here can support more robust risk assessment and reduction for future lava flow events, on the Island of Hawai'i and elsewhere.

Declarations

Competing interests The authors declare no competing interests.

References

Andronico D, Branca S, Calvari S, Burton M, Caltabiano T, Corsaro RA, Del Carlo P, Garfi G, Lodato L, Miragila L, Murè F, Neri M, Pecora E, Pompilio M, Salerno G, Spampinato L (2005) A multi-disciplinary study of the 2002–03 Etna eruption: Insights into a complex plumbing system. Bull Volcanol 67:314–330. https://doi.org/10.1007/s00445-004-0372-8

Applied Technology Council (1985) Earthquake damage evaluation data for California. Applied Technology Council

Applied Technology Council (2005) ATC 20-2 rapid evaluation safety assessment form. Applied Technology Council. Available at: https://www.atcouncil.org/atc-20. Accessed 14 Nov 2019

Aramaki S, Hayakawa Y, Fujii T, Nakamura K, Fukuoka T (1986) The October 1983 eruption of Miyakejima volcano. J Volcanol Geotherm Res 29:203–229. https://doi.org/10.1016/0377-0273(86)90045-4

Babb J, Kauahikaua J, Tilling R (2011) The story of the Hawaiian Volcano Observatory—a remarkable first 100 years of tracking eruptions and earthquakes: U.S. Geological Survey General Information Product 135. U.S. Geological Survey. Available at: https://pubs.usgs.gov/gip/135/

Bachèlery P, Morin J, Villeneuve N, Soulé H, Nassor H, Ali AR (2016) Structure and eruptive history of Karthala volcano. In: Active volcanoes of the southwest Indian Ocean 345–366. Springer, Berlin, Heidelberg. https://doi.org/10.1007/978-3-642-31395-0_22

Barberi F, Brondi F, Carapezza ML, Cavarra L, Murgia C (2003) Earthen barriers to control lava flows in the 2001 eruption of Mt. Etna. Journal of Volcanology and Geothermal Research. https://doi.org/10.1016/S0377-0273(03)00038-6

Baxter PJ, Allard P, Halbwachs M, Komorowski J-C, Woods AW, Ancia A (2002) Human health and vulnerability in the Nyiragongo volcano crisis Democratic Republic of Congo. Acta Vulcanol 14:109–114

Baxter P, Boyle R, Cole P, Neri A, Spence R, Zuccaro G (2005) The impacts of pyroclastic surges on buildings at the eruption of the Soufrière Hills volcano, Montserrat. Bull Volcanol 67:292–313. https://doi.org/10.1007/s00445-004-0365-7

Big Island Now (2018) Extended power outages in lower Puna. Big Island Now. Available at: https://bigislandnow.com/2018/05/29/extended-power-outages-will-affect-lower-puna/. Accessed 21 Feb 2021

Blong RJ (1984) Volcanic hazards: a sourcebook on the effects of eruptions. Academic Press, Australia

Blong R (2003a) A review of damage intensity scales. Nat Hazards 29:57–76. https://doi.org/10.1023/A:1022960414329

Blong R (2003b) Building damage in Rabaul, Papua New Guinea, 1994. Bull Volcanol 65:43–54

Bonaccorso A, Calvari S, Boschi E (2016) Hazard mitigation and crisis management during major flank eruptions at Etna volcano: Reporting on real experience. In: Harris AJL, De Groeve T, Garel F, Carn SA (eds) Detecting, modelling and responding to effusive eruptions. Geological Society London, Special Publications (IAVCEI) Series 426. https://doi.org/10.1144/SP426.4

Bracker M (1944) Vesuvius erupts, swallows town after allies evacuate its people; San Sebastiano, on volcano's slope, buried under tons of molten rock—witness says flow behaved capriciously (Published 1944). Nytimes.com. Available at: https://www.nytimes.com/1944/03/21/archives/vesuvius-erupts-swallows-town-after-allies-evacuate-its-people-san.html. Accessed 4 Feb 2021

Brantley SR, Kauahikaua JP, Babb JL, Orr TR, Patrick MR, Poland MP, Trusdell FA, Oliveira D, Garcia MO, Camp VE, Grunder A (2019) Communication strategy of the US Geological Survey Hawaiian Volcano Observatory during the lava-flow crisis of 2014 2015, Kīlauea Volcano, Hawai'i. Field Volcanology: a Tribute to the Distinguished Career of Don Swanson 538:351–373

Brown SK, Jenkins SF, Sparks RSJ, Odbert H, Auker MR (2017) Volcanic fatalities database: Analysis of volcanic threat with distance and victim classification. J Appl Volcanol 6:15. https://doi.org/10.1186/s13617-017-0067-4

CBS (2018) Man says lava bomb from Hawaii volcano "snapped" his leg in half. CBSNews.com. Available at: https://www.cbsnews.com/news/hawaii-Kīlauea-volcano-lava-bomb-injury-darryl-clinton/. Accessed 20 Feb 2021

Charvet I, Suppasri A, Kimura H, Sugawara D, Imamura F (2015) A multivariate generalized linear tsunami fragility model for Kesennuma City based on maximum flow depths, velocities and debris impact, with evaluation of predictive accuracy. Nat Hazards 79:2073–2099. https://doi.org/10.1007/s11069-015-1947-8

Civil Defense (2018) Community questions from the 9/5/18 meeting in Pāhoa with county of Hawai'i responses. Available at: http://records.hawaiicounty.gov/weblink/1/edoc/96058/2018-09-05%20Questions%20Answers%20Eruption%20Community%20Meeting.pdf. Accessed 21 Feb 2021

Copernicus Emergency Management Service (2021) [EMSR546] La Palma: grading product, monitoring 63, version 1, release 1, RTP map #02. Available at: https://emergency.copernicus.eu/mapping/ems-product-component/EMSR546_AOI01_GRA_MONIT63_r1_RTP02/1. Accessed 18 Mar 2022

County of Hawai'i (2008) Puna community development plan. Available at: https://www.hawaiicountycdp.info/puna-cdp/draft-plan-recommendations/1%20Puna%20CDP%20amended%20Nov-2011.pdf/view. Accessed 21 Feb 2021

County of Hawai'i (2018) Mandatory evacuation order rescinded. Available at: http://records.hawaiicounty.gov/weblink/1/doc/95865/Page1.aspx. Accessed 21 Feb 2021

County of Hawai'i News (2019) Highway 132 paving finished. Available at: https://www.hawaiicounty.gov/Home/Components/News/News/145/720. Accessed 8 Mar 2022

County of Hawai'i (2020) Kīlauea recovery and resilience plan. Available at: https://recovery.hawaiicounty.gov/home/showpublisheddocument?id=302781. Accessed 21 Feb 2021

County of Hawai'i (2021) County of Hawai'i Real Property Tax Office. Available at: http://www.hawaiipropertytax.com/. Accessed 5 Apr 2019

Del Negro C, Fortuna L, Vicari A (2005) Modelling lava flows by cellular nonlinear networks (CNN): Preliminary results. Nonlinear Process Geophys 12:505–513

Dieterich HR, Patrick MR, Diefenbach AK, Lundgren P, Cashman KV, Grant GE (2019) December. Lava effusion rates and channel dynamics during the 2018 Kīlauea lower East Rift Zone eruption. In: AGU Fall Meeting Abstracts (V43C-0215)

Dieterich H, Diefenbach A, Soule S, Zoeller M, Patrick M, Major J, Lundgren P (2021) Lava effusion rate evolution and erupted volume during the 2018 Kīlauea lower East Rift Zone eruption. Bull Volcanol. https://doi.org/10.1007/s00445-021-01443-6

Dolling K, Chu PS, Fujioka F (2005) A climatological study of the Keetch/Byram drought index and fire activity in the Hawaiian Islands. Agric Meteorol 133:17–27. https://doi.org/10.1016/j.agrformet.2005.07.016

Dong L, Shan J (2013) A comprehensive review of earthquake-induced building damage detection with remote sensing techniques. ISPRS J Photogramm Rem Sens 84. https://doi.org/10.1016/j.isprsjprs.2013.06.011

Douglas J (2007) Physical vulnerability modelling in natural hazard risk assessment. Natural Hazards Earth Syst Sci 7:283–288. https://doi.org/10.5194/nhess-7-283-2007

Favalli M, Pareschi MT, Neri A, Isola I (2005) Forecasting lava flow paths by a stochastic approach. Geophys Res Letters. https://doi.org/10.1029/2004GL021718

Friedland CJ, Levitan ML (2009) Loss-consistent categorization of hurricane wind and storm surge damage for residential structures. In: Proceedings of the 11th Americas Conference on Wind Engineering, San Juan, Puerto Rico

Gansecki C, Lee RL, Shea T, Lundblad SP, Hon K, Parcheta C (2019) The tangled tale of Kīlauea's 2018 eruption as told by geochemical monitoring. Sci 1212:1–9. https://doi.org/10.1126/science.aaz0147

Global Volcanism Program (1976) Report on Karangetang (Indonesia). In: Squires D (ed) Natural Science Event Bulletin 1:13. Smithsonian Institution. https://doi.org/10.5479/si.GVP.NSEB197610-267020

Global Volcanism Program (1977a) Report on Nyiragongo (DR Congo). In: Squires D (ed) Natural Science Event Bulletin 2:3. Smithsonian Institution. https://doi.org/10.5479/si.GVP.NSEB197703-223030

Global Volcanism Program (1977b) Report on Piton de la Fournaise (France). In: Squires D (ed) Natural Science Event Bulletin 2:4. Smithsonian Institution

Global Volcanism Program (1981) Report on Etna (Italy). In: McClelland L (ed) Scientific Event Alert Network Bulletin 6:3. Smithsonian Institution. https://doi.org/10.5479/si.GVP.SEAN198103-211060

Global Volcanism Program (1983) Report on Etna (Italy). In: McClelland L (ed) Scientific Event Alert Network Bulletin 8:7. Smithsonian Institution. https://doi.org/10.5479/si.GVP.SEAN198307-211060

Global Volcanism Program (1992) Report on Kīlauea (United States). In: McClelland L (ed) Bulletin of the Global Volcanism Network 17:12. Smithsonian Institution. https://doi.org/10.5479/si.GVP.BGVN199212-332010

Global Volcanism Program (2021a) Report on Nyiragongo (DR Congo). In: Bennis KL, Venzke E (eds) Bulletin of the Global Volcanism Network 46:6. Smithsonian Institution. https://doi.org/10.5479/si.GVP.BGVN202106-223030

Global Volcanism Program (2021b) Report on Pacaya (Guatemala). In: Crafford AE Venzke E (eds) Bulletin of the Global Volcanism Network 46:6. Smithsonian Institution. https://doi.org/10.5479/si.GVP.BGVN202106-342110

Gregg CE (2005) Natural hazards in Hawai'i: Some studies of awareness, risk perceptions and preparedness. University of Hawai'i at Manoa

Harris A, Rowland S (2001) FLOWGO: a kinematic thermo-rheological model for lava flowing in a channel. Bull Volcanol 63:20–44. https://doi.org/10.1007/s004450000120

Harris AJL (2015) Basaltic lava flow hazard. In: Volcanic hazards, risks, and disasters 17–46. https://doi.org/10.1016/B978-0-12-396453-3.00002-2

Hartung C, Lerer A, Anokwa Y, Tseng C, Brunette W, Borriello G (2010) Open data kit: tools to build information services for developing regions. In: Proceedings of the 4th ACM/IEEE international conference on information and communication technologies and development 1–12

Hawaii Wildfire Management Organization (2013) Hawaii Wildfire Management Organization communities at risk from wildfire map. Available at: https://static1.squarespace.com/static/5254fbe2e4b04bbc53b57821/t/54ff7277e4b03d629b8d254a/1426027145261/County+of+Hawaii+%28East%29+Community+Hazard+Assessment+Maps.pdf. Accessed 21 Feb 2021

Hawaii State Energy Office (2018) Hawaii energy facts and figures. Available at: http://energy.hawaii.gov/wp-content/uploads/2018/06/HSEO_2018_EnergyFactsFigures.pdf. Accessed 24 Apr 2022

Hayes JL, Calderón R, Deligne NI, Jenkins SF, Leonard GS, McSporran AM, Williams GT, Wilson TM (2019) Timber-framed building damage from tephra fall and lahar: 2015 Calbuco eruption, Chile. J Volcanol Geotherm Res 374:142–159. https://doi.org/10.1016/j.jvolgeores.2019.02.017

HELCO (2020) Puna Geothermal Venture back online after 2½ years, sends power to Hawaii Island grid. Hawaiianelectric.com. Available at: https://www.hawaiianelectric.com/puna-geothermal-venture-back-online-after-two-and-a-half-years-sends-power-to-hawaii-island-grid. Accessed 21 Feb 2021

Hon K, Kauahikaua J, Denlinger R, Mackay K (1994) Emplacement and inflation of pāhoehoe sheet flows: observations and measurements of active lava flows on Kīlauea volcano. Hawaii Geol Soc Am Bull 106:351–370. https://doi.org/10.1130/0016-7606(1994)106%3C0351:EAIOPS%3E2.3.CO;2

Isshiki N (1964) Mode of eruption of Miyake-jima volcano in historic times. Bull Volcanol 27:29–48

Jacobs J (2018) Lava bomb hits tourist boat in Hawaii, injuring 23. Nytimes.com. Available at: https://www.nytimes.com/2018/07/17/us/lava-bomb-boat-video-hawaii.html. Accessed 22 Feb 2021

Jenkins S, Komorowski J, Baxter P, Spence R, Picquout A, Lavigne F, Surono, (2013) The Merapi 2010 eruption: an interdisciplinary impact assessment methodology for studying pyroclastic density current dynamics. J Volcanol Geotherm Res 261:316–329. https://doi.org/10.1016/j.jvolgeores.2013.02.012

Jenkins SF, Spence RJS, Fonseca JFBD, Solidum RU, Wilson TM (2014) Volcanic risk assessment: quantifying physical vulnerability in the built environment. J Volcanol Geotherm Res 276:105–120. https://doi.org/10.1016/j.jvolgeores.2014.03.002

Jenkins SF, Phillips JC, Price R, Feloy K, Baxter PJ, Hadmoko DS, de Bélizal E (2015) Developing building-damage scales for lahars: application to Merapi volcano. Indonesia Bull Volcanol. https://doi.org/10.1007/s00445-015-0961-8

Jenkins SF, Day SJ, Faria BE, Fonseca JFBD (2017) Damage from lava flows: insights from the 2014–2015 eruption of Fogo, Cape Verde. J Appl Volcanol 6:1–17. https://doi.org/10.1186/s13617-017-0057-6

Kern C, Lerner AH, Elias T, Nadeau PA, Holland L, Kelly PJ, Werner CA, Clor LE, Cappos M (2020) Quantifying gas emissions associated with the 2018 rift eruption of Kīlauea Volcano using ground-based DOAS measurements. Bull Volcanol 82:1–24. https://doi.org/10.1007/s00445-020-01390-8

Kilburn CRJ (2015) Lava flow hazards and modeling. In: The encyclopedia of volcanoes, 957–969. Academic Press. https://doi.org/10.1016/b978-0-12-385938-9.00055-9

Kim K, Pant P, Yamashita E, Ghimire J (2019) Analysis of transportation disruptions from recent flooding and volcanic disasters in Hawai'i. Transp Res Rec 2673:194–208. https://doi.org/10.1177/0361198118825460

Kircher CA, Nassar AA, Kustu O, Holmes WT (1997) Development of building damage functions for earthquake loss estimation. Earthq Spectra 13:663–682. https://doi.org/10.1193/2F1.1585974

Komorowski J C, Morin J, Jenkins S, Kelman I (2016) Challenges of volcanic crises on small islands states. In: Observing the volcano world, 353–371. https://doi.org/10.1007/11157_2015_15

Koshimura Shunichi, Moya Luis, Mas EricK, Bai Yanbing et al (2020) Tsunami Damage Detection with Remote Sensing: A Review. Geosciences. https://doi.org/10.3390/geosciences10050177

Krafft M (1982) L'éruption volcanique du Karthala en Avril 1977 (Grande Comore, océan Indien). Comptes Rendus Académie Sciences 294:753–758

Lallemant D, Kiremidjian A, Burton H (2015) Statistical procedures for developing earthquake damage fragility curves. Earthq Eng Struct Dyn 44:1373–1389. https://doi.org/10.1002/eqe.2522

Living with Volcanoes (2008) Volcanic eruptions on Miyakejima island in 2000. Available at: https://volcanoes.usgs.gov/vsc/file_mngr/file-169/miyakejima_english.pdf. Accessed 28 Mar 2021

Longo BM, Grunder A, Chuan R, Rossignol A (2005) SO2 and fine aerosol dispersion from the Kilauea plume, Kau district, Hawaii, USA. Geol 33:217–220. https://doi.org/10.1130/G21167.1

Ludwig KA, Pennaz A, Wilkins AM (2019) Results from the Department of the Interior Strategic Sciences Group technical support for the 2018 Kīlauea eruption. US Department of the Interior. Available at: http://pubs.er.usgs.gov/publication/70205097

McDaniel S, Loh R, Dale S, Smith K, Vaidya M (2008) Rehabilitation of 'ōhi'a-swordfern (metrosideros polymorpha-nephrolepis multiflora) woodlands following the kupukupu fire, Hawaii Volcanoes National Park

Macdonald GA (1962) The 1959 and 1960 eruptions of Kīlauea volcano, Hawaii, and the construction of walls to restrict the spread of the lava flows. Bull Volcanol 24:249–294. https://doi.org/10.1007/BF02599351

Macdonald GA, Eaton JP (1964) Hawaiian volcanoes during 1955. US Geol Surv Bull 1171:1–170

Macdonald GA, Abbott A, Peterson FL (1983) Volcanoes in the sea: the geology of Hawaii. University of Hawaii Press

Mactagone MK (2019) A growing breathing home: a responsive design to single-family homes in Hawaii (Doctoral dissertation, University of Hawai'i at Manoa)

Mattox TN, Heliker C, Kauahikaua J, Hon K (1993) Development of the 1990 Kalapana flow field, Kīlauea volcano. Hawaii Bull Volcanol 55:407–413. https://doi.org/10.1007/BF00302000

Moore RB, Helz RT, Dzurisin D, Eaton GP, Koyanagi RY, Lipman PW, Puniwai GS (1980) The 1977 eruption of Kilauea volcano. Hawaii J Volcanol Geotherm Res 7:189–210. https://doi.org/10.1016/0377-0273(80)90029-3

Morin J, Lavigne F (2009) Institutional and social responses to hazards related to Karthala volcano, Comoros. Part 2: Deep-seated root causes of Comorian vulnerabilities. Shima: The Int J Res Isl Cult 3:54–71

Morgan AV (2000) The Eldfell eruption, Heimaey, Iceland: a 25-year retrospective. Geosci Can 27:11–18

Mossoux S, Kervyn M, Canters F (2019) Assessing the impact of road segment obstruction on accessibility of critical services in case of a hazard. Nat Hazards Earth Syst Sci 19:1251–1263. https://doi.org/10.5194/nhess-19-1251-2019

Neal CA, Brantley SR, Antolik L, Babb JL, Burgess M, Calles K, Cappos M, Chang JC, Conway S, Desmither L, Dotray P (2019) The 2018 rift eruption and summit collapse of Kīlauea Volcano. Sci 363:367–374. https://doi.org/10.1126/science.aav7046

Nofal OM, Van De Lindt JW, Do TQ, Yan G, Hamideh S, Cox DT, Dietrich JC (2021) Methodology for regional multihazard hurricane damage and risk assessment. J Struct Engineer 147:04021185

Nolan ML (1972) The towns of the volcano: a study of the human consequences of the eruption of Parícutin volcano. Texas A&M University

NPS (2018) Volcanic activity and earthquakes keep most of park closed. National Park Service. Available at: https://www.nps.gov/havo/learn/news/20180806_pr_closure.htm. Accessed 20 Feb 2021

Office of Planning (2020) Hawaii statewide GIS program. Department of Business Economic Development, State of Hawaii. Available at: http://hawaii.gov/dbedt/gis/. Accessed 5 Aug 2019

Office of the Governor (2021) 2018 Kīlauea eruption fissure 8 officially named. Available at: https://governor.hawaii.gov/newsroom/dbedt-news-release-2018-kilauea-eruption-fissure-8-officially-named/. Accessed 30 Mar 2022

Okinaka (2018) Life after lava: restoring a community. Hawaiian Electric. Available at: https://medium.com/@PoweringHawaii/life-after-lava-restoring-a-community-557e57d3ec2c. Accessed 20 Feb 2021

OSM (2017) Open Street Map. Available at: http://www.openstreetmap.org/. Accessed 5 Aug 2019

Patrick M, Orr T, Fisher G, Trusdell F, Kauahikaua J (2017) Thermal mapping of a pāhoehoe lava flow, Kīlauea Volcano. J Volcanol Geotherm Res 332:71–87. https://doi.org/10.1016/j.jvolgeores.2016.12.007

Patrick MR, Parcheta C, Dietterich HR (2018) Evolution of the Fissure 8 lava flow on Kilauea's Lower East Rift Zone. In: AGU Fall Meeting Abstracts (V21B-01)

Patrick MR, Dietterich HR, Lyons JJ, Diefenbach AK, Parcheta C, Anderson KR, Namiki A, Sumita I, Shiro B, Kauahikaua JP (2019) Cyclic lava effusion during the 2018 eruption of Kīlauea Volcano. Sci 366:1–10. https://doi.org/10.1126/science.aay9070

Patrick M, Johanson I, Shea T, Waite G (2020a) The historic events at Kīlauea Volcano in 2018: summit collapse, rift zone eruption, and M w 6.9 earthquake: preface to the special issue. Bull Volcanol 82:46. https://doi.org/10.1007/s00445-020-01377-5

Patrick MR, Houghton BF, Anderson KR, Poland MP, Montgomery-Brown E, Johanson I, Thelen W, Elias T (2020b) The cascading origin of the 2018 Kīlauea eruption and implications for future forecasting. Nat Commun 11:5646. https://doi.org/10.1038/s41467-020-19190-1

Patrick MR, Dietterich HR, Parcheta CE, Zoeller M, Carr BB (2020c) New insights into lava flow dynamics during the 2018 eruption of Kīlauea. In: AGU Fall Meeting Abstracts 2020c Dec (V002-0009)

Patrick MR, Orr TR, Swanson D, Houghton BF, Wooten KM, Desmither L, Parcheta C, Fee D (2021) Kīlauea's 2008–2018 summit lava lake—chronology and eruption insights. In: Patrick MR, Orr T, Swanson D, Houghton BF (eds) The 2008–2018 summit lava lake at Kīlauea volcano, Hawai'i. U.S. Geological Survey Professional Paper 1867, p 50. https://doi.org/10.3133/pp1867A

Peiris N (2006) Vulnerability functions for tsunami loss estimation. In: First European conference on earthquake engineering and seismology. Geneva, Switzerland 3–8

Poland M, Orr TR, Kauahikaua JP, Brantley SR, Babb JL, Patrick MR, Neal CA, Anderson KR, Antolik L, Burgess M, Elias T, Fuke S, Fukunaga P, Johanson IA, Kagimoto M, Kamibayashi K, Lee L, Miklius A, Million W, Moniz C, Okubo PG, Sutton AJ, Takahashi TJ, Thelen WA, Tollett W, Trusdell FA (2016) The 2014–2015 Pāhoa lava flow crisis at Kīlauea Volcano, Hawai'i: Disaster avoided and lessons learned. GSA Today 26:4–10. https://doi.org/10.1130/GSATG262A.1

Proctor CR, Lee J, Yu D, Shah AD, Whelton AJ (2020) Wildfire caused widespread drinking water distribution network contamination. AWWA Water Sci 2:1183. https://doi.org/10.1002/aws2.1183

Rose AN, McKee J, Urban ML, Bright EA (2018) LandScan 2017. Available at: https://landscan.ornl.gov/

Ruangrassamee A, Yanagisawa H, Foytong P, Lukkunaprasit P, Koshimura S, Imamura F (2006) Investigation of tsunami-induced damage and fragility of buildings in Thailand after the December 2004 Indian Ocean tsunami. Earthq Spectra 22:377–401. https://doi.org/10.1193/1.2208088

Smith C, Tunison, J (1992) Fire and alien plants in Hawaii: research and management implications for native ecosystems. Alien plant invasions in native ecosystems of Hawaii: management and research. Cooperative National Park Resources Studies Unit, Honolulu 394–408

Spence RJS, Pomonis A, Baxter PJ, Coburn AW, White M, Dayrit M (1996) Building damage caused by the Mt. Pinatubo eruption of June 14 –15, 1991. In: Newhall CG, Punongbayan R (eds) Fire and mud: Eruptions and lahars of mount Pinatubo. University of Washington Press, Phillipines

Staudacher T, Peltier A, Ferrazzini V, Di Muro A, Boissier P, Catherine P, Kowalski P, Lauret F, Lebreton J (2016) Fifteen years of intense eruptive activity (1998–2012) at Piton de la Fournaise volcano (La Réunion): a review. In: Bachèlery P, Lénat JF, Di Muro A, Michon L (eds) Active volcanoes of the Southwest Indian Ocean: Piton de la Fournaise and Karthala. Actives volcanoes of the world. Springer, Berlin 139–170. https://doi.org/10.1007/978-3-642-31395-0_9

Swanson DA, Rose TR, Mucek AE, Garcia MO, Fiske RS, Mastin LG (2014) Cycles of explosive and effusive eruptions at Kīlauea Volcano, Hawai'i. Geol 42:631–634. https://doi.org/10.1130/G35701.1

The Guardian (2018) Hawaii power plant shut down as lava nears geothermal wells. The Guardian. Available at: https://www.theguardian.com/us-news/2018/may/22/hawaii-puna-geothermal-venture-power-plant-shut-down-as-lava-nears-geothermal-wells. Accessed 21 Feb 2021

Thompson D (2018) The lava dwellers, Big Island, Hawai'i: these people live on one of the most active volcanoes on earth. Honolulu magazine. Available at: https://www.honolulumagazine.com/the-lava-dwellers-big-island-hawaii-these-people-live-on-one-of-the-most-active-volcanoes-on-earth/. Accessed 20 Feb 2021

Tilling RI, Heliker C, Swanson DA (2010) Eruptions of Hawaiian volcanoes; past, present and future. USGS Gen Inf Prod 117:63. https://doi.org/10.3133/gip117

Tomiczek T, Kennedy A, Zhang Y, Owensby M, Hope ME, Lin N, Flory A (2017) Hurricane damage classification methodology and fragility functions derived from Hurricane Sandy's effects in coastal New Jersey. J Water Port Coast Ocean Engineer 143:04017027. https://doi.org/10.1061/(ASCE)WW.1943-5460.0000409

Tsang SW, Lindsay JM (2020) Lava flow crises in inhabited areas part I: Lessons learned and research gaps related to effusive, basaltic eruptions. J Appl Volcanol 9:1–26. https://doi.org/10.1186/s13617-020-00096-y

Tsang SW, Lindsay JM, Kennedy B, Deligne NI (2020) Thermal impacts of basaltic lava flows to buried infrastructure: workflow to determine the hazard. J Appl Volcanol 9:1–8

U.S. Geological Survey (2013) Volcano Watch — Mauna Ulu—an opportunity to study a long-lived rift zone eruption. Available at: https://www.usgs.gov/center-news/volcano-watch-mauna-ulu-opportunity-study-a-long-lived-rift-zone-eruption. Accessed 11 Jun 2021

U.S. Geological Survey (2018) Preliminary summary of Kīlauea Volcano's 2018 lower East Rift Zone. Available at: https://prd-wret.s3.us-west-2.amazonaws.com/assets/palladium/production/atoms/files/PrelimSum_LERZ-Summit_2018.pdf. Accessed 20 Nov 2020

U.S. Geological Survey (2020a) Simplified table of Kīlauea historical activity modified from Macdonald and others (1983). Kīlauea Historical Activity Table. Available at: https://prd-wret.s3.us-west-2.amazonaws.com/assets/palladium/production/atoms/files/HVO_website_Kil_historical_activity_table_2020a0604.pdf. Accessed 18 Mar 2021

U.S. Geological Survey (2020b) November 23, 2020b—Kīlauea 2018 lower East Rift Zone lava flow thicknesses. Available at: https://www.usgs.gov/node/278815. Accessed 27 Apr 2021

Wardman JB, Sword-Daniels VL, Stewart C, Wilson TM (2012) Impact assessment of the May 2010 eruption of Pacaya volcano, Guatemala. GNS Science Report 2012/009

Wantim MN, Bonadonna C, Gregg CE, Menoni S, Frischknecht C, Kervyn M, Ayonghe SN (2018) Forensic assessment of the 1999 Mount Cameroon eruption, West-Central Africa. J Volcanol Geotherm Res 1:13–30. https://doi.org/10.1016/j.jvolgeores.2018.06.007

Whitty RC, Ilyinskaya E, Mason E, Wieser PE, Liu EJ, Schmidt A, Roberts T, Pfeffer MA, Brooks B, Mather TA, Edmonds M (2020) Spatial and temporal variations in SO_2 and $PM_{2.5}$ levels around Kīlauea volcano, Hawai'i during 2007–2018. Front Earth Sci 8:36. https://doi.org/10.3389/feart.2020.00036

WHO (2011) WHO guidelines for drinking-water quality, 4th edn. World Health Organization, Geneva

Williams RS, Moore JG (1983) Man against volcano: the eruption on Heimaey, Vestmennaeyjar, Iceland. Report U.S. Geological Survey Unnumbered Series General Interest Publication 1–26. Available at: http://pubs.usgs.gov/gip/heimaey/

Williams GT, Jenkins SF, Biass S, Wibowo HE, Harijoko A (2020) Remotely assessing tephra fall building damage and vulnerability: Kelud Volcano, Indonesia. J Appl Volcanol 9:1–18. https://doi.org/10.1186/s13617-020-00100-5

Wilson TM, Stewart C, Sword-Daniels V, Leonard GS, Johnston DM, Cole JW, Wardman J, Wilson G, Barnard ST (2012) Volcanic ash impacts on critical infrastructure. Phys Chem Earth 45:5–23. https://doi.org/10.1016/j.pce.2011.06.006

Wilson G, Wilson TM, Deligne NI, Cole JW (2014) Volcanic hazard impacts to critical infrastructure: a review. J Volcanol Geotherm Res 286:148–182. https://doi.org/10.1016/j.jvolgeores.2014.08.030

Wright TL, Chun JY, Esposo J, Heliker C, Hodge J, Lockwood JP, Vogt SM (1992) Map showing lava-flow hazard zones, Island of Hawaii. US Geological Survey. Available at: https://pubs.usgs.gov/mf/1992/2193/

Witmer FDW (2015) Remote sensing of violent conflict: eyes from above. International Journal of Remote Sensing. https://doi.org/10.1080/01431161.2015.1035412

Zoeller MH, Perroy RL, Wessels RL, Fisher GB, Robinson JE, Bard JA, Peters J, Mosbrucker AR, Parcheta CE (2020) Geospatial database of the 2018 lower East Rift Zone eruption of Kīlauea Volcano, Hawai'i: U.S. Geological Survey data release. https://doi.org/10.5066/P9S7UQKQ